# 1

# Thin-Film Photovoltaics as a Mainstream of Solar Power Engineering

Leonid A. Kosyachenko
*Chernivtsi National University*
*Ukraine*

## 1. Introduction

Provision of energy is one of the most pressing problems facing humanity in the 21st century. Without energy, it is impossible to overcome the critical issues of our time. Industrial world suggests continuous growth in energy consumption in the future.
According to the U.S. Department of Energy, the world's generating capacity is now close to 18 TW. The main source of energy even in highly developed countries is fossil fuel, i.e. coal, oil and natural gas. However, resources of fossil fuel are limited, and its production and consumption irreversibly affect the environmental conditions with the threat of catastrophic climate change on Earth. Other energy sources, particularly *nuclear* energy, are also used that would fully meet *in principle* the energy needs of mankind. Capacity of existing nuclear reactors (nearly 450 in the world) is ~ 370 GW. However, increasing their capacity up to ~ 18 TW or about 50 times (!), is quite problematic (to provide humanity with *electric* energy, the capacity of nuclear power should be increased about 10 times). Resources of hydroelectric, geothermal, wind energy, energy from biofuels are also limited. At the same time, the power of solar radiation of the Earth's surface exceeds the world's generating capacity by more than 1000 times. It remains only to master this accessible, inexhaustible, gratuitous and nonhazardous source of energy in an environmentally friendly way.
Solar energy can be converted into heat and electricity. Different ways of converting sunlight into electricity have found practical application. The power plants, in which water is heated by sunlight concentrating devices resulting in a high-temperature steam and operation of an electric generator, are widespread. However, solar cells are much more attractive due to the *direct* conversion of solar radiation into electricity. This is the so-called *photovoltaics.* Under the conditions of the growing problems of global warming, photovoltaics is the most likely candidate to replace fossil fuels and nuclear reactors.

## 2. Silicon solar cells

Over the decades, solar modules (panels) based on single-crystalline (mono-crystalline, c-Si), polycrystalline (multi-crystalline, mc-Si), ribbon (ribbon-Si) and amorphous (a-Si) silicon are dominant in photovoltaics (Fig. 1).
In recent years, photovoltaics demonstrates high growth rates in the entire energy sector. According to the European Photovoltaic Industry Association , despite the global financial and economic crisis, the capacity of installed solar modules in the world grew by 16.6 GW in

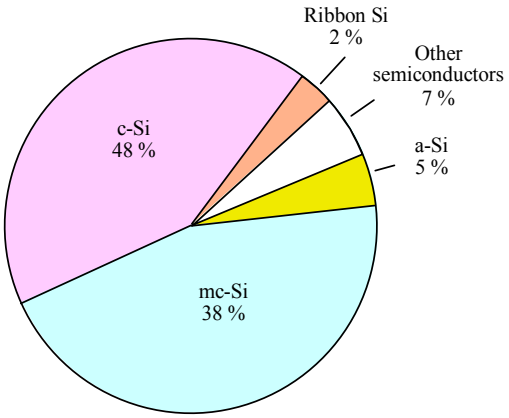


Fig. 1. Distribution of capacity of photovoltaic energy in the world.

2010, and their total capacity reached ~ 40 GW, that is almost 8 times more than in 2005. The growth rate of the photovoltaic energy for the next 4-5 years is expected to be quite high. In 2014, capacity of installed modules will be about 14 GW and 30 GW according to the pessimistic and optimistic forecast, respectively. Nevertheless, despite the relatively high annual growth, the contribution of semiconductor solar cells in the global energy system is small (less than 0.3%!), and the prospects for *desired rapid* development of photovoltaics are not reassuring (Fig. 2). The contribution of Si photovoltaic solar power plants in generation capacity in the world will reach ~ 1% only in the years 2018-2020, and may exceed 10% in the years 2045-2050 (EPIA, 2011; EUR 24344 PV, 2010; Jager-Waldau, 2010). Analysts do not accept the development of the PV scenario shown by the dashed line in Fig. 2. Thus, solving the energy problems by developing Si photovoltaics seems too lengthy.[1]

The reason for the slow power growth of traditional silicon solar modules lies in a large consumption of materials and energy, high labor intensiveness and, as a consequence, a low productivity and high cost of modules with acceptable photovoltaic conversion efficiency for mass production (16-17 and 13-15% in the case of single-crystalline and polycrystalline material, respectively) (Szlufcik et al., 2003; Ferrazza, 2003).[2] The problem is fundamental and lies in the fact that silicon is an i*ndirect* semiconductor and therefore the *total* absorption needs its significant thickness (up to 0.5 mm and more). As a result, to collect the charge photogenerated in a thick absorbing layer, considerable diffusion length of minority carriers (long lifetime and high mobility) and, therefore, high quality material with high *carrier diffusion length of hundreds of micrometers* are required.

Estimating the required thickness of the semiconductor in solar cells, one is often guided by an effective penetration depth of radiation into the material $\alpha^{-1}$, where $\alpha$ is the absorption coefficient in the region of electronic interband transitions. However, the value of $\alpha$ varies

[1] In the European Union, these rates are much higher. Now the cumulative power of solar modules is 1.2% and, by 2015 and 2020, will rise to 4-5% and 6-12% of the EU's electricity demand, respectively.

[2] A lot of effort has been undertaken to increase the efficiency of silicon solar cells above 20-24% but improvements are reached only with the help of cost-intensive processes, which usually cannot be implemented into industrial products (Koch et al., 2003).

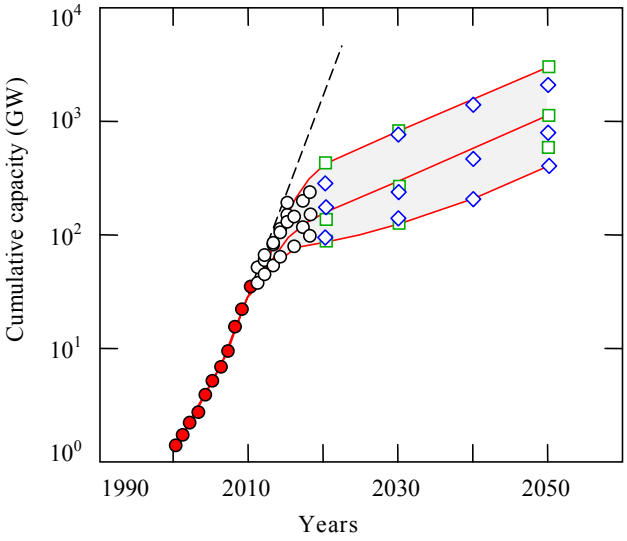


Fig. 2. Evolution of world cumulative installed PV capacity until 2050: ● historical data, ○, □, ◇ forecasts (EPIA, 2011; EUR 24344 PV, 2010; Hegedus & Luque, 2011).

rather widely, especially in the indirect semiconductor, and solar radiation is distributed over the spectrum in a complicated manner (Fig. 3(a)). Therefore, the absorptive capacity (absorptivity) of the material, used in solar cell, can be described by a certain *integral* characteristic, which takes into account the absorption spectrum of the material and the spectral distribution of solar radiation. For a structure with flat surfaces, the integral absorption ability of the radiation, which has penetrated into the material (certain part of radiation is reflected from the front surface), can be represented as

$$A(d) = \frac{\sum_i \frac{\Phi_i + \Phi_{i-1}}{2}\left[1 - \exp\left(-\frac{\alpha_i + \alpha_{i-1}}{2} d\right)\right]\Delta\lambda_i}{\sum_i \frac{\Phi_i + \Phi_{i-1}}{2}\Delta\lambda_i}, \quad (1)$$

where $\Phi_i$ is the spectral power density of solar radiation at the wavelength $\lambda_i$ under standard solar irradiation AM1.5 shown in Fig. 3(a), $\Delta\lambda_i$ is the spacing between neighboring wavelengths in Table 9845-1 of the International Organization for Standardization (Standard ISO, 1992), and $\alpha_i$ is the absorption coefficient at wavelength $\lambda_i$. The summation in Eq. (1) is made from $\lambda \approx$ 300 nm to $\lambda = \lambda_g = hc/E_g$, since at wavelengths $\lambda$ shorter than 300 nm, terrestrial radiation of the Sun is virtually absent, and when $\lambda > \lambda_g$, radiation is not absorbed in the material with the generation of electron-hole pairs.

Fig. 3(b) shows the dependences of absorptivity of solar radiation $A$ of single-crystalline silicon on the thickness of the absorber layer $d$ calculated by Eq. (1).

As seen in Fig. 3(b), in crystalline silicon, the total absorption of solar radiation in the fundamental absorption region ($h\nu \geq E_g$) occurs when $d$ is close to 1 cm (!), and 95% of the radiation is absorbed at a thickness of about 300 μm. More absorption can be achieved by using the reflection of light from the rear surface of the solar cell, which is usually completely

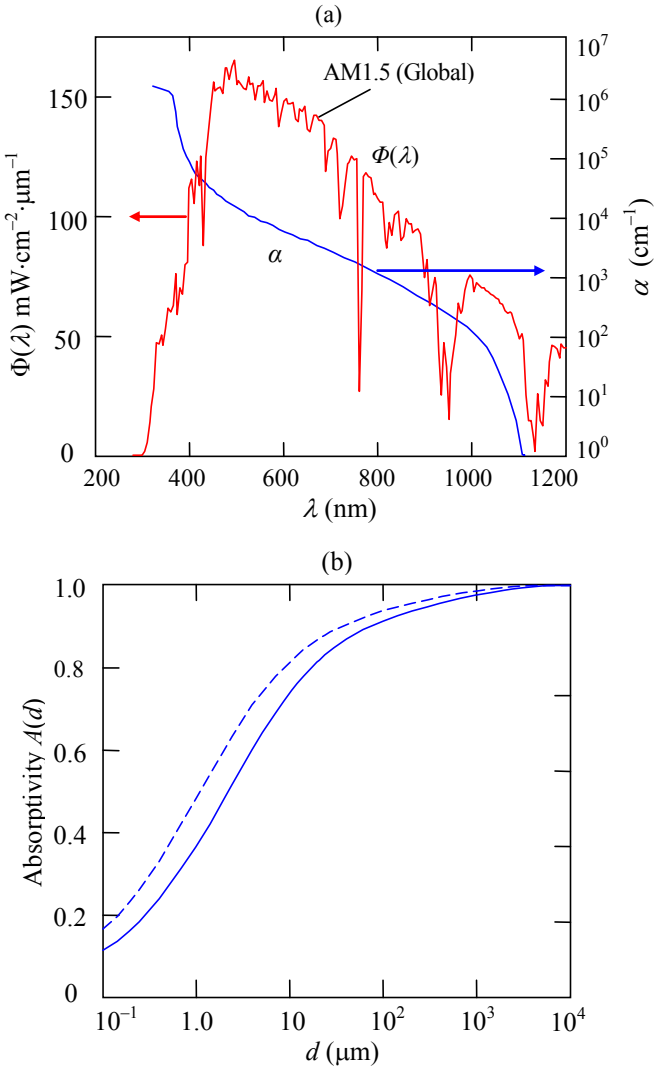


Fig. 3. (a) – Power spectral density of the total solar radiation Φ under AM1.5 conditions and the absorption curve $\alpha(\lambda)$ for crystalline silicon. (b) – Dependence of absorptivity of solar radiation in the $h\nu \geq E_g$ spectral range on the absorber layer thickness $d$ for crystalline silicon. The dashed line shows the absorptivity of a silicon wafer taking into account 100% reflection from its rear surface.

covered with metal. If in the ideal case, the reflectivity of light from the rear surface is unity, the absorption of the plate will be such as if its thickness is twice as much. In this case, 95% of the radiation is absorbed by the plate of 150 μm thickness.

Of course, it has to be rejected to use silicon wafers of thickness a few millimeters, so that the absorption of solar radiation was complete. Many companies producing silicon modules

agreed on a compromise thickness of 150-250 μm, when about 93% of solar radiation with photon energy $h\nu \geq E_g$ is absorbed or about 94% when the rear surface of the solar cell is mirror (Szlufcik et al., 2003; Ferrazza, 2003).[3] Deficiency of absorption in the material offsets by the creation of a special profile on surfaces (texturing) and by other ways. Needless to say, an anti-reflective coating is applied to reduce significantly the reflection from the front surface because over 30% of the radiation is reflected from a flat silicon surface.

Production of solar modules based on silicon wafers involves a lot of stages (Hegedus & Luque, 2011). The so-called metallurgical grade (MG) silicon is obtained from quarzite ($SiO_2$) with charcoal in a high-temperature arc furnace. Then MG silicon is highly purified commonly by a method developed by the Siemens Company consisting of the fractional distillation of chlorosilanes. Finally, chlorosilanes are reduced with hydrogen at high temperatures to produce the so-called semiconductor grade (SG) silicon. By recrystallizing such polycrystalline silicon, single-crystalline Si ingots are often grown by the Czochralski (Cz) or the floating-zone (FZ) techniques adapted from the microelectronics industry. This is followed by cutting (slicing) the ingot into wafers, of course, with considerable waste. It should be noted that the cost of silicon purification, production of ingots, slicing them into wafers constitute up to 40-55% of the cost of solar module.

Manufacture of conventional silicon solar cell also includes a number of other operations. Among them, (i) chemical etching wafers to provide removal of the layer damaged during slicing and polishing; (ii) high-temperature diffusion to create a p-n junction; (iii) anisotropic etching to build a surface structure with random pyramids that couples the incoming light more effectively into the solar cell; (iv) complicated procedure of applying full area and grid-like ohmic contacts to p- and n-type regions provided a minimum of electrical and recombination losses (contacts in silicon solar cells are often made by screen-printing metal paste, which is then annealed at several hundred degrees Celsius to form metal electrodes), etc. (Mauk, et al., 2003). Once the cells are manufactured they are assembled into modules either in the cell factories or in module assembly factories that purchase cells from variety cell factories (Hegedus & Luque, 2011). All that complicates the manufacturing technology and, hence, reduces the productivity and increases the cost of solar modules.

Summing up, one should again emphasize that single-crystalline Si modules are among the most efficient but at the same time the most expensive since they require the highest purity silicon and involve a lot of stages of complicated processes in their manufacture.

For decades, an intensive search for cheaper production technology of silicon solar cells is underway. Back in the 1980's, a technology of material solidification processes for production of large silicon ingots (blocks with weights of 250 to 300 kg) of **polycrystalline** (**multicrystalline**) **silicon** (mc-Si) has been developed (Koch et al., 2003). In addition to lower cost manufacturing process, an undoubted advantage of mc-Si is the rational use of the material in the manufacture of solar cells due to the rectangular shape of the ingot. In the case of a single-crystalline ingot of cylindrical form, the so-called "pseudo-square" wafers with rounded corners are used, i.e. c-Si modules have some gaps at the four corners of the cells).

Polycrystalline silicon is characterized by defects caused by the presence of random grains of crystalline Si, a significant concentration of dislocations and other crystal defects (impurities). These defects reduce the carrier lifetime and mobility, enhance recombination of carriers and ultimately decrease the solar cells efficiency. Thus, polysilicon-based cells

[3] Further thinning of silicon is also constrained by the criteria of mechanical strength of a wafer as well as the handling and processing techniques (silicon is brittle).

are less expensive to produce single-crystalline silicon cells but are less efficient. As a result, cost per unit of generated electric power ("specific" or "relative" cost) for c-Si and mc-Si modules is practically equal (though the performance gap has begun to close in recent years). The polysilicon-based cells are the most common solar modules on the market being less expensive than single-crystalline silicon.

A number of methods for growing the so-called **ribbon-Si**, i.e. a polycrystalline silicon in the form of thin sheets, is also proposed. The advantages of ribbon silicon are obvious, as it excludes slicing the ingot into thin wafers, allowing material consumption to reduce roughly *halved*. However, the efficiency of ribbon-Si solar cells is not as high as of mc-Si cells because the need of high quality material with the thickness of the absorber layer of 150-250 μm and, hence, with high carrier diffusion lengths of hundreds of micrometers remains (Hegedus & Luque, 2011). Nevertheless, having a lower efficiency, ribbon-Si cells save on production costs due to a great reduction in waste because slicing silicon crystal into the thin wafers results in losses (of about 50%) of expensive pure silicon feedstock (Koch et al., 2003). Some of the manufacturing technologies of silicon ribbons are introduced into production, but their contribution to the Si-based solar energy is negligible (Fig. 1). The cost of ribbon-Si modules, as well as other types of silicon solar modules, remains quite high.

Many companies are developing solar cells that use lenses or/and mirrors to concentrate a large amount of sunlight onto a small area of photovoltaic material to generate electricity. This is the so-called **concentrated photovoltaics**. The main gain that is achieved through the involvement of concentrators is to save material. This, however, does not too reduce the cost of the device, because a number of factors lead to higher prices. (i) For the concentration of radiation, an optical system is necessarily required, which should maintain a solar cell in focus by the hardware when the sun moves across the sky. (ii) With a significant increase in the intensity of the radiation, the photocurrent also increases significantly, and the electrical losses rapidly increase due to voltage drop across the series-connected resistance of the bulk of the diode structure and contacts. (iii) For the removal of heat generated by irradiation that decreases the efficiency of photovoltaic conversion, it is necessary to use copper heatsinks. (iv) The requirements to quality of the solar cell used in the concentrator considerably increase. (v) Using concentrators, only direct beam of solar radiation is used, which leads to losing about 15% efficiency of solar module.

Nevertheless, today the efficiency of solar concentrators is higher compared to conventional modules, and this trend will intensify in the application of more efficient solar devices. In 2009, for example, the power produced in the world using solar energy concentration did not exceed 20-30 MW, which is ~ 0.1% of silicon power modules (Jager-Waldau, 2010). According to experts, concentrator market share can be expected to remain quite small although increasing by 25% to 35% per year (Von Roedern, 2006).

In general, in this protracted situation, experts and managers of some silicon PV companies have long come to conclusion that there would be limits to growing their wafer (ribbon) silicon business to beyond 1 GW per year by simply expanding further (Von Roedern, 2006). All of these companies are researching wafer-Si alternatives including the traditional *thin-film technologies* and are already offering such commercial thin-film modules.

Concluding this part of the analysis, one must agree, nevertheless, that wafer and ribbon silicon technology provides a fairly high rate of development of solar energy. According to the European Photovoltaic Industry Association (EPIA), the total installed PV capacity in the world has multiplied by a factor of 27, from 1.5 GW in 2000 to 39.5 GW in 2010 – a yearly growth rate of 40% (EPIA, 2011).

Undoubtedly, solar cells of all types on silicon wafers, representatives of the so-called *first generation photovoltaics*, will maintain their market position in the future. In hundreds of companies around the world, one can always invest (with minimal risk) and implement the silicon technology developed for microelectronics with some minor modifications (in contrast, manufacturers of thin-film solar modules had to develop their "own" manufacturing equipment). Monocrystalline and polycrystalline wafers, which are used in the semiconductor industry, can be made into efficient solar cells with full confidence. It is also important that silicon is very abundant, clean, nontoxic and very stable. However, due to limitations in production in large volumes of silicon for solar modules, which are both highly efficient and cost-effective, often-expressed projections for *desirable significant* increase in their contribution to the world energy system in the coming years are highly questionable.

## 3. Thin-film solar cells

Among the radical ways to reduce the cost of solar modules and to increase drastically the volume of their production is the transition to thin-film technology, the use of direct-gap semiconductors deposited on a cheap large-area substrate (glass, metal foil, plastic).

We start with the fact that the direct-gap semiconductor can absorb solar radiation with a thickness, which is much smaller than the thickness of the silicon wafer. This is illustrated by the results of calculations in Fig. 4 similar to those performed for the single-crystalline silicon shown in Fig. 2. Calculations were carried out for direct-gap semiconductors, which is already used as absorber layers of solar modules: a-Si, CdTe, $CuInSe_2$ and $CuGaSe_2$.

As expected, the absorptivity of solar radiation of direct-gap semiconductors in general is much stronger compared to crystalline silicon but the curves noticeably differ among themselves (in the references, the absorption curves for a-Si are somewhat different). Almost complete absorption of solar radiation by amorphous silicon (a-Si) in the $\lambda \leq \lambda_g = hc/E_g$ spectral range is observed at its thickness $d$ > 30-60 μm, and 95% of the radiation is absorbed at a thickness of 2-6 μm (Fig. 4(a)). These data are inconsistent with the popular belief that in a-Si, as a direct-gap semiconductor, the *total* absorption of solar radiation occurs at a layer thickness of several microns. The total absorption of solar radiation in CdTe occurs if the thickness of the layer exceeds 20-30 μm, and 95% of the radiation is absorbed if the layer is thinner than ~ 1 μm. Absorptivities of the $CuInSe_2$ and $CuGaSe_2$ are even higher. Almost complete absorption of radiation in these materials takes place at a layer thickness of 3-4 μm, and 95% of the radiation is absorbed if the thickness of layer is only 0.4-0.5 μm (!).

Thus, the transition from crystalline silicon to direct-gap semiconductors leads to noncomparable less consumption of photoelectrically active material used in the solar cell.

High absorptivity of a semiconductor has important consequences with respect to other characteristics of the semiconductors used in solar cells. Since the direct-gap semiconductor can absorb solar radiation at its thickness much smaller than the thickness of the silicon wafer (ribbon), the requirements for chemical purity and crystalline perfection of the absorber layer in the solar cell became much weaker.

In fact, to collect photogenerated charge carriers, it is necessary to have a diffusion length of minority carriers in excess of the thickness of the absorbing layer. In the case of crystalline Si, the photogenerated carriers must be collected at a thickness of 1-2 hundred microns and 2 orders of magnitude smaller than in the case of CdTe, CIS or CGS. From this it follows that in the solar cell based on direct-gap semiconductor, the diffusion length $L$ may be about two

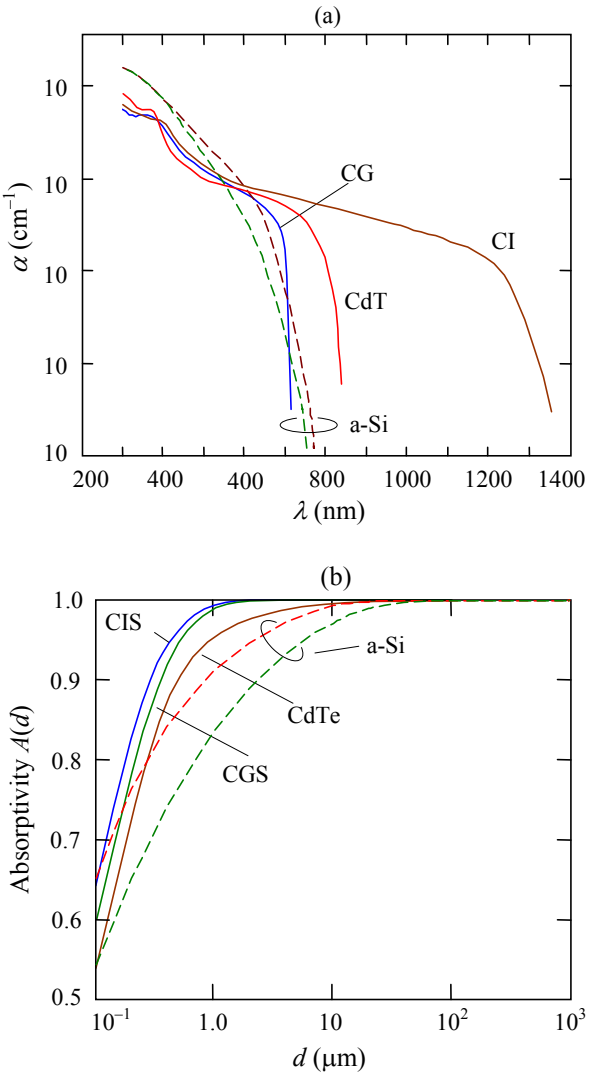


Fig. 4. Absorption curves (a) and dependence of absorptivity of AM1.5 solar radiation in the $h\nu \geq E_g$ spectral range on the absorber layer thickness $d$ (b) for amorphous silicon (a-Si), cadmium telluride (CdTe), copper-indium diselenide (CIS) and copper gallium diselenide (CGS) (Han et al., 2007; Paulson et al., 2003; Gray et al., 1990; http://refractiveindex.info/a-Si).

orders of magnitude smaller, i.e. the carrier lifetime $\tau$ can be by 4(!) order shorter ($L \sim \tau^{1/2}$). Thus, the manufacture of thin film solar modules based on the direct-gap semiconductors does not require costly high purification and crystallinity of the material as it is needed in the production of modules based on crystalline, multicrystalline or ribbon silicon.

Thin-film technology has a number of other significant merits. While Si devices are manufactured from wafers or ribbons and then processed and assembled to form a modules,

in thin-film technology many cells are simultaneously made and formed as a module. The layers of solar cells are deposited sequentially on moving substrates in a continuous highly automated production line (conveyor system) and, importantly, at temperatures not exceeding 200-650°C compared with 800-1450°C for the main processes of c-Si. This minimises handling and facilitates automation leading to the so-called *monolithic integration*.[4] Thin-film solar modules offer the lowest manufacturing costs, and are becoming more prevalent in the industry because allow to improve manufacturability of the production at significantly larger scales than for wafer or ribbon Si modules. Therefore, it is generally recognised that the contribution of thin-film technology in solar energy will be to grow from year to year faster. Many analysts believe *that it is only a matter of time before thin films would replace silicon wafer-based solar cells as the dominant photovoltaic technology*.

Unquestionable leaders in thin film technologies are solar cells on **amorphous silicon** (a-Si), **copper-indium-gallium diselenide** ($CuIn_xGa_{1-x}Se_2$) and **cadmium telluride** (CdTe), whose market share is expanding every year (Hegedus & Luque, 2011). The rest of the thin-film technologs are yet too immature to appear in the market but some of them is already reaching the level of industrial production. Below these technologies will first be briefly described, and a more detailed analysis of solar modules based on a-Si, CdTe and CIGS are allocated in separate subsections. Now the most successful non-Si based thin film PV technologies are representatives of the so-called *second generation photovoltaics* $CuIn_xGa_{1-x}Se_2$ and CdTe solar cells. Both of them have been manufactured in large scale and are commercialized.

(i) For a long time, intensive researches on own initiative and within different levels of government programs are carried out on developing **thin-film crystalline Si solar cells**. These devices are opposed to solar cells based on silicon wafers or ribbons because are made by depositing thin silicon layer on a foreign substrate. The thickness of such a layer can vary from a few tens of nanometers to tens of micrometers. Thin-film solar cells based on **crystalline silicon on glass substrate** (**CSG**) occupy a special place in these studies (Basore, 2006; Widenborg & Aberle, 2007). Such devices have the potential to reduce considerably the cost of manufacture of photovoltaic modules due to a significant thinning the absorbing layer and the use of cheap glass substrates. Of course, in a thin layer and a thick wafer of silicon, processes of collection of photogenerated carriers may substantially differ due to differences not only of layer thickness but also the structure of the material and its parameters such as the lifetime of carriers, their mobility and others. Because the mobility and lifetime of charge carriers in thin-film silicon layers are relatively low, the carrier diffusion lengths are generally lower than the penetration depths for the long-wavelength part of the solar spectrum and a narrow p-n junction cannot be employed in the thin-film silicon case. For this reason, one has to use p-i-n diode structures, where the photo-generation takes place in the i-layer and transport and collection are drift-assisted (Shah et al., 2006).

All the same, the thickness of Si layer is of great importance for other reasons. If in a typical case, the Si thickness is less than ~ 2 μm, an effective optical enhancement technique (light trapping) is necessary. Indeed, approximately only half of the solar radiation is absorbed in such layer, even when eliminating the reflection from the front surface of the solar cell (Fig. 3(b)).

[4] For example, First Solar manufactures the CdTe-based modules (120 cm × 60 cm, 70-80 W) on high throughput, automated lines from semiconductor deposition to final assembly and test – all in one continuous process. The whole flow, from a piece of glass to a completed solar module, takes less than 2.5 hours.

One effective way to obtain light trapping is to texture the supporting material (glass substrate) prior to the deposition of the Si film. To implement this idea, in particular, a glass aluminium-induced texturing (AIT) method was developed (Widenborg & Aberle, 2007).
On the textured surface, silicon is deposited in amorphous form followed by solid-phase crystallisation and hydrogen passivation. An amorphous silicon is transformed into a polycrystalline layer after a special annealing at 400-600ºC. As a result of the texture, light is transmitted obliquely into the Si film, significantly enhancing the optical pathlength and thus increasing the optical absorption. The effect is further enhanced by depositing a high-quality reflector onto the back surface. Best optical absorption is obtained if the texture and the back surface reflector are optimised such that the total internal reflection occurs both at the front and the rear surface of the Si film, enabling multiple passes of the light through the solar cell. There are other glass texturing methods compatible with producing poly-Si thin-film solar cells, for example, CSG Solar's glass bead method (Ji & Shi, 2002). Apart from the light trapping benefits, the textured substrate also reduces reflection losses at the front surface of the solar cell.
It should be noted again that the development of silicon solar cells on glass substrate is not limited to the problem of light trapping. Fabrication of these modules is also facing serious problems of differences in the thermal expansion coefficients of silicon and substrate, the influence of substrate material on the properties of a silicon thin layer at elevated temperatures and many others.
Despite the efforts of scientists and engineers for about 30 years, the stabilized efficiency of typical CSG devices still does not exceed 9-10%. Nevertheless, large-area CSG modules with such efficiency produce sufficient power to provide installers with a cost-effective alternative to conventional wafer or ribbon Si based products. Because of a low cost of production even with reduced efficiency, large-area CSG modules are attractive for some applications and are in production in factories having a capacity of tens of MW per year (Basore, 2006).
(ii) **Dye-sensitized-solar-cells** (DSSCs), invented by M. Grätzel and coworkers in 1991, are considered to be extremely promising because they are made of low-cost materials with simple inexpensive manufacturing procedures and can be engineered into flexible sheets (O'Regan & Grätzel, 1991; Grätzel, 2003; Chiba et al., 2006).
DSSCs are emerged as a truly new class of energy conversion devices. Mechanism of conversion of solar energy into electricity in these devices is quite peculiar. Unlike a traditional solar cell design, dye molecules in DSSC absorb sunlight, just as it occurs in nature (like the chlorophyll in green leaves). A porous layer of nanocrystalline oxide semiconductor (very often $TiO_2$) provides charge collection and charge separation, which occurs at the surfaces between the dye, semiconductor and electrolyte. In other words, the natural light harvest in photosynthesis is imitated in DSSC. DSSCs are representatives of the *third generation solar technology*. The dyes used in early solar cells were sensitive only in the short-wavelength region of the solar spectrum (UV and blue). Current DSSCs have much wider spectral response including the long-wavelength range of red and infrared radiation. It is necessary to note that DSSCs can work even in low-light conditions, i.e. under cloudy skies and non-direct sunlight collecting energy from the lights in the house.
The major disadvantage of the DSSC design is the use of the liquid electrolyte, which can freeze at low temperatures. Higher temperatures cause the liquid to expand, which causes problems sealing of the cell. DSSCs with liquid electrolyte can have the less long-term stability due to the volatility of the electrolyte contained organic solvent. Replacing the liquid electrolyte with a solid has been a field of research.

It should be noted that DSSCs can degrade when exposed to ultraviolet radiation. However, it is believed that DSSCs are still at the start of their development stage. Efficiency gain is possible and has recently started to be implemented. These include, in particular, the use of quantum dots for conversion of higher-energy photons into electricity, solid-state electrolytes for better temperature stability, and more.

Although the light-to-electricity conversion efficiency is less than in the best thin film cells, the DSSC price should be low enough to compete with fossil fuel electrical generation. This is a popular technology with some commercial impact forecast especially for some applications where mechanical flexibility is important. As already noted, energy conversion efficiencies achieved are low, however, it has improved quickly in the last few years. For some laboratory dye-sensitized-solar-cells, the conversion efficiency of 10.6% under standard AM 1.5 radiation conditions has been reached (Grätzel, 2004).

(iii) **Organic solar cells** attract the attention also by the simplicity of technology, leading to inexpensive, large-scale production. In such devices, the organic substances (polymers) are used as thin films of thickness ~ 100 nm. Unlike solar cells based on inorganic materials, the photogenerated electrons and holes in organic solar cells are separated not by an electric field of p-n junction. The first organic solar cells were composed of a single layer of photoactive material sandwiched between two electrodes of different work functions (Chamberlain, 1983). However, the separation of the photogenerated charge carriers was so inefficient that far below 1% power-conversion efficiency could be achieved. This was due to the fact that photon absorption in organic materials results in the production of a mobile excited state (exciton) rather than free electron-hole pairs in inorganic solar cells, and the exciton diffusion length in organic materials is only 5-15 nm (Haugeneder et al., 1999). Too short exciton diffusion length and low mobility of excitons are factors limiting the efficiency of organic solar cell, which is low in comparison with devices based on inorganic materials.

Over time, two dissimilar organic layers (bilayer) with specific properties began to be used in the organic solar cell (Tang, 1986). Electron-hole pair, which arose as a result of photon absorption, diffuses in the form of the exciton and is separated into a free electron and a hole at the interface between two materials. The effectiveness of ~ 7% reached in National Renewable Energy Laboratory, USA can be considered as one of best results for such kind of solar cells (1-2% for modules). However, instabilities against oxidation and reduction, recrystallization and temperature variations can lead to device degradation and lowering the performance over time. These problems are an area in which active research is taking place around the world. Organic photovoltaics have attracted much attention as a promising new thin-film PV technology for the future.

(iv) Of particular note are solar cells based on **III-V group semiconductors such as GaAs** and AlGaAs, GaInAs, GaInP, GaAsP alloys developed in many laboratories. These multi-junction cells consist of multiple thin films of different materials produced using metalorganic vapour phase epitaxy. Each type of semiconductor with a characteristic band gap absorbs radiation over a portion of the spectrum. The semiconductor band gaps are carefully chosen to generate electricity from as much of the solar energy as possible.

GaAs-based multi-junction devices were originally designed for special applications such as satellites and space exploration. To date they are the most efficient solar cells (higher than 41% under solar concentration and laboratory conditions), but the issue of large-scale use of GaAs-based solar cells in order to solve global energy problems is not posed (King, 2008; Guter at al., 2009).

Other solar cells have also been suggested, namely quantum dots, hot carrier cells, etc. However, they are currently studied at the cell-level and have a long way to be utilized in large-area PV modules.

### 3.1 Amorphous silicon

Amorphous silicon (a-Si) has been proposed as a material for solar cells in the mid 1970's and was the first material for commercial thin-film solar cells with all their attractiveness to reduce consumption of absorbing material, increase in area and downturn in price of modules.

It was discovered that the electrical properties of a-Si deposited from a glow discharge in silane ($SiH_4$) are considerably different from single-crystalline silicon (Deng & Schiff, 2003). When put into silane of a small amount of phosphine ($PH_3$) or boron ($B_2H_6$), electrical conduction of a-Si becomes n-type or p-type, respectively (Spear & Le Comber, 1975).

In 1976 Carlson and Wronski reported the creation of a-Si solar cells with efficiency of 2.4% using p-i-n structure deposited from a glow discharge in silane rather than evaporating silicon (Carlson & Wronski, 1976). The maximum efficiency of thin film amorphous silicon solar cells was estimated to be 14–15%.

a-Si is an allotropic form of silicon, in which there is no far order characteristic of a crystal. Due to this, some of a-Si atoms have nonsaturated bonding that appears as imperfection of the material and significantly affects its properties. The concentration of such defects is reduced by several orders due to the presence of hydrogen, which is always present in large quantities when obtained from the silane or at the surface treatment by hydrogen. The hydrogen atoms improve essentially the electronic properties of the plasma-deposited material. This material has generally been known as *amorphous hydrogenated silicon* (a-Si:H) and applied in the majority in practice.

Depending on the gas flow rate and other growth conditions, the optical band gap of a-Si:H varies, but typically ranges from 1.6 to 1.7 eV. Its absorption coefficient is much higher than that of mono-crystalline silicon (Fig. 4). As it has been noted, in the case of a-Si:H, the thickness of 2-6 μm (rather than 300 μm as in the case of c-Si) is sufficient for almost complete (95%) absorption of solar radiation in the $h\nu \geq E_g$ spectral range. It is also important that the technology of a-Si:H is relatively simple and inexpensive compared to the technologies for growing Si crystals. The low deposition temperature (< 300°C) and the application of the monolithic technique for a-Si:H module manufacturing were generally considered as key features to obtain low costs of the devices.

As in the past, the layers of a-Si:H can be deposited on large area (1 $m^2$ or more) usually by method termed as plasma enhanced chemical vapor deposition (PECVD) on glass coated with transparent conductive oxide (TCO) or on non-transparent substrates (stainless steel, polymer) at relatively low temperatures (a-Si:H can be also deposited roll-to-roll technology). Like the crystalline silicon, a-Si:H can be doped creating p-n junctions, which is widely used in other field of electronics, particularly in thin-film transistors (TFT).

This opens up the possibility of relatively easy to form the desired configuration of the active photodiode structure of the solar cell. To date, p-i-n junction is normally used in solar cells based on a-Si:H. The i-layer thickness is amount to several hundred nanometers, the thickness of frontal p-film, which is served as a "window" layer, is equal to ~ 20 nm, the back n-layer can be even thinner. It is believed that almost all electron-hole pairs are photogenerated in the i-layer, where they are separated by electric field of p-i-n structure. The output power of a-Si:H solar cell can has a *positive temperature coefficient*, i.e. at elevated ambient temperatures the efficiency is higher.

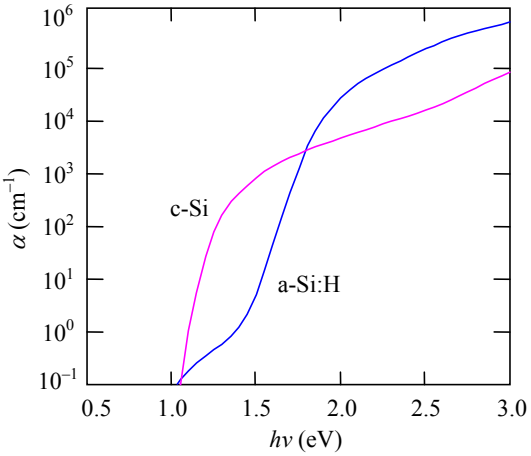


Fig. 5. Spectral dependence of absorption coefficient *a* in the crystalline (c-Si) and amorphous hydrogenated silicon (a-Si: H).

Quite common in commercial solar cells are the **multi-layer structures** based on amorphous silicon and silicon germanium alloys, when the p-i-n photodiode structures (subcells) with different band gap semiconductors are superimposed one layer on another. It seemed that the spectrum splitting tandem structure, a representative of the *third generation of solar cells*, opened the prospect of developing highly efficient and low-cost solar cells (Kuwano et al. 1982).

One of the tandem a-Si:H structures is shown in Fig. 6. This is the so-called superstrate design, when solar radiation enters through the transparent substrate such as glass or polymer (the substrate design with flexible stainless steel foil is also widely used). In the superstrate design, p- , i- and n-layers of a-Si:H are consistently applied on a glass plate coated with a transparent film (ITO, $SnO_2$). Over them the analogous layers of a-SiGe:H alloy are deposited in the discharge of silane $CH_4$ together with $GeH_4$. The frontal 0.5-μm thick layers of p-i-n structure absorb photons with energies larger than ~ 1.9 eV and transmits photons with energies lower than ~ 1.9 eV. The band gap of a-SiGe:H alloy is lower than that of a-Si, therefore the radiation that has passed through a-Si will be absorbed in the a-SiGe layers, where additional electron-hole pairs are generated and solar cell efficiency increases. Even greater effect can be achieved in a triple-junction structure a-Si/a-SiGe/a-SiGe. One of the record efficiency of such solar cell is 14.6% (13.0% stabilized efficiencies) (Yang et al,. 1997). At high content of Ge in $Si_{1-x}Ge_x$ alloy, optoelectronic properties of the material are deteriorated, therefore in multi-junction solar cells, the band gap of the amorphous $Si_{1-x}Ge_x$ layers cannot be less than 1.2-1.3 eV.

The results presented in Fig. 4, show that 10-15% of solar radiation power in the range $h\nu > E_g$ is not absorbed if the thickness of the a-Si layer is 1 μm. Therefore, to improve the power output, back reflector and substrate texturing can be used in a-Si solar cells. Apparently, the light trapping occurs for weakly absorbed light. It was shown that using geometries maximizing enhancement effects, the short circuit current in amorphous silicon solar cell (< 1 μm thick) increases by several mA/cm² (Deckman et al., 1983).

The use of multi-junction solar cells is successful because there is no need for lattice matching of materials, as is required for crystalline heterojunctions.

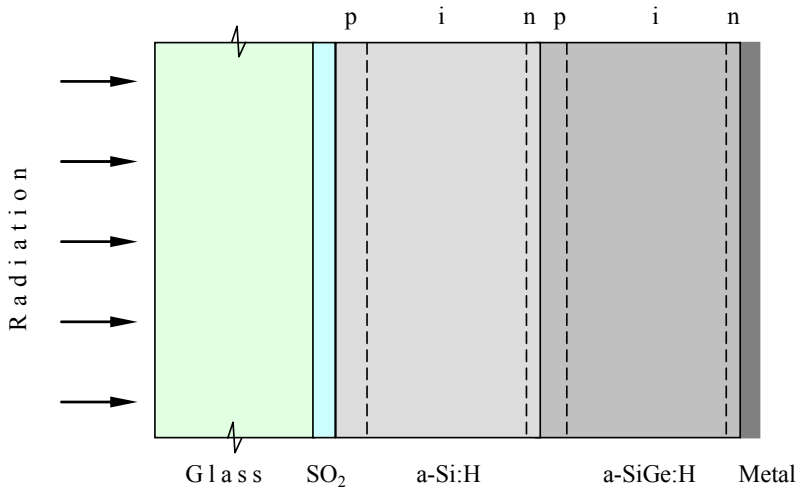


Fig. 6. Tandem solar cell based on a-Si:H and a-SiGe:H (Deng & Schiff, 2003).

Solar cells based on a-Si:H are much cheaper than those produced on silicon wafers or ribbons, but their efficiency in operation under illumination becomes lower during the first few hundred hours and then the degradation process is slowed down considerably (Fig. 7). The degradation of multiple-junction and single-junction solar cells is usually in the range of 10-12 and 20-40%, respectively (20-30% for commercial devices).
Degradation of a-Si:H solar cells, called the Staebler–Wronski effect, is a *fundamental* a-Si property. The same degradation is observed in solar cells from different manufacturers and with different initial efficiencies (Von Roedern et al., 1995). It has been established that stabilization of the degradation occurs at levels that depend on the operating conditions, as well as on the operating history of the modules. After annealing for several minutes at 130-150°C, the solar cell properties can be restored. The positive effect of annealing can also occur

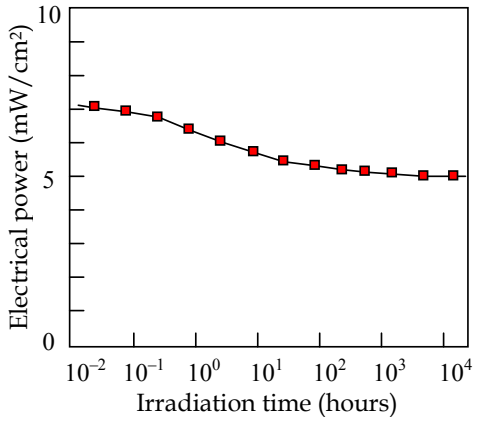


Fig. 7. Decline in power output of solar cell based on a-Si:H in the initial period of irradiation 100mV/sm² (Staebler–Wronski effect) (Deng & Schiff, 2003).

as a result of *seasonal* temperature variations therefore the efficiency of a-Si:H modules in the summer is greater than in winter.

Degradation of a-Si:H solar cells is mostly caused by photostimulated formation of defects (dangling bonds) that act as recombination centers (Staebler & Wronski, 1977). The effect can not be explained by a single degradation mechanism. At least two mechanisms have to be involved: a fast one that can be annealed at typical module operating temperatures, and a slow one that does not recover measurably when annealing temperatures are limited to values below 70°C (Von Roedern et al., 1995; Von Roedern & del Cueto, 2000).

It is important from a practical point of view that a-Si:H reaches a "stabilized" state after extended irradiation. The stabilized a-Si:H arrays show less than 1% degradation per year, which is about the same rate at which crystalline silicon losses power over time. Therefore, still 20 years ago, it was recommended that all a-Si solar cells and modules performances should be reported after stabilization under standard conditions for 1000 hours at 50°C (Von Roedern & del Cueto, 2000).

Along with amorphous silicon, during the same 30 years, the intensive investigations of the possibility of using the glow discharge method for producing **thin-film crystalline silicon** were also carried out (Faraji et al., 1992; Meier et al., 1994). In 1994, using this method thin-film p-i-n solar cells based on hydrogenated **microcrystalline silicon** (**μc-Si**) have been prepared at substrate temperatures as low as ~ 200°C (Meier et al., 1994). Compared with a-Si:H solar cells, an enhanced absorption in the near-infrared (up to 1.1 eV) and an efficiency of 4.6% were obtained. First light-soaking experiments indicate also no degradation for such μc-Si:H cells. Years later, other groups started research activities utilizing this material and naming the microcrystalline silicon as "**nanocrystalline**" (**nc-Si**) or "**policrystalline**" **silicon** (**poly-Si**).

Microcrystalline silicon (μc-Si, nc-Si,poly-Si) has small grains of crystalline silicon (< 50 nm) within the amorphous phase. This is in contrast to multi-crystalline silicon, which consists solely of crystalline silicon grains separated by grain boundaries. Microcrystalline silicon has a number of useful advantages over a-Si, because it can have a higher electron mobility due to the presence of the silicon crystallites. It also shows increased absorption in the red and infrared regions, which makes μc-Si as an important material for use in solar cells. Another important advantages of μc-Si is that it has improved stability over a-Si, one of the reasons being because of its lower hydrogen concentration. There is also the advantage over poly-Si, since the μc-Si can be deposited using conventional low temperature a-Si deposition techniques, such as plasma enhanced chemical vapor deposition.

Special place in the thin-film photovoltaics is the so-called **micromorph solar cells**, which are closely related to the amorphous silicon. The term "micromorph" is used for stacked tandem thin-film solar cells consisting of an a-Si p-i-n junction as the top component, which absorbs the "blue" light, and a μc-Si p-i-n junction as the bottom component, which absorbs the "red" and near-infrared light in the solar spectrum (Fig. 8). This artificial word has first been mentioned by Meier in the late 1990's (Meier et al., 1995; Meier et al., 1998).

A double-junction or tandem solar cell consisting of a microcrystalline silicon solar cell ($E_g$ = 1.1 eV) and an amorphous silicon cell ($E_g \approx$ 1.75 eV) corresponds almost to the theoretically optimal band gap combination. Using μc-Si:H as the narrow band gap cell instead of a-SiGe cell yields the higher efficiency in the long-wavelength region. At the same time, the stable μc-Si:H bottom cell contributes to usually a better stability of the entire micromorph tandem cell under light-soaking. The stabilized efficiency of such double-junctions solar cells of 11-12% was achieved (Meier et al., 1998).

It was also suggested that the micromorph solar cells open new perspectives for low-temperature thin-film crystalline silicon technology and even has the potential to become for the next third generation of thin-film solar cells (Keppner et al., 1999). However, due to the effect of the indirect band, the μc-Si component of solar cells requires much thicker i-layers to absorb the sunlight (1.5 to 2 μm compared to 0.2 μm thickness of a-SiGe:H absorber). At the same time, the deposition rate for μc-Si:H material is significantly lower compared to that for a-SiGe, so that a much longer time is needed to deposit a thicker μc-Si layer than what is needed for an a-SiGe structure. In addition, advanced light enhancement schemes need to be used because μc-Si has a lower absorption coefficient. Finally, μc-Si solar cell has a lower open-circuit voltage compared to a-SiGe:H cell.
Nevertheless, one should tell again that micromorph tandem solar cells consisting of a microcrystalline silicon bottom cell and an amorphous silicon top cell are considered as one of the promising thin-film silicon solar-cell devices. The promise lies in the hope of simultaneously achieving high conversion efficiencies at relatively low manufacturing costs.

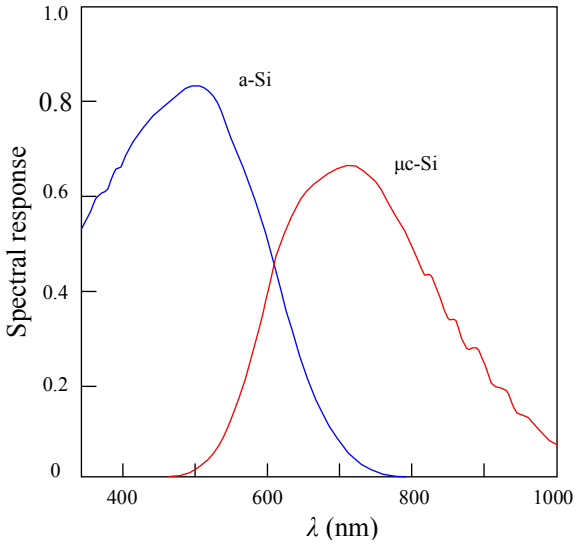


Fig. 8. Spectral response of a double-stacked micromorph tandem solar cell (Keppner et al., 1999).

Concluding the section, one must admit the considerable progress for more than 30 years in improving the efficiency of a-Si and micromorph solar cells. However, despite the persistent efforts of researchers and engineers in various laboratories in many countries, under initiatory researches and government programs, stabilized efficiency of large-area a-Si:H solar modules lies within 8 to 10%. So far, stabilized efficiencies of about 11-12% can be obtained with micromorph solar cells. A number of technological methods allow the efficiency just somewhat to increase using the above alloys of Si-Ge and special multiple-junction structures including the use of μc-Si:H and others.[5] But the cost of such multiple-

[5] One of the highest stabilized cell efficiency for a laboratory triple-junction structure is ~ 13.0% (Deng & Schiff, 2003).

junction solar cells always increases markedly. In addition, faster deposition processes need to be developed that is necessary for low-cost and high-throughput manufacturing.
Thus, in the field of amorphous and micromorph silicon photovoltaics, it is succeeded in realizing only part of the benefits of thin-film solar cells, and its share in the global solar energy is quite small (Fig. 1). The use of a-Si:H and micromorph solar cells is limited preferably to areas where low cost is more important than the efficiency of photoelectric conversion (such as consumer electronics). Semitransparent modules are also used as architectural elements or windows and skylights. This is the so-called building-integrated photovoltaics (BIPV), where large building envelope areas can be covered with the PV modules available at the lowest prices per square meter. The advantage of BIPV is also that the initial cost can be offset by reducing the amount spent on building materials. This trend becomes noticeable segment of the photovoltaic industry.

### 3.2 Copper-indium-gallium diselenide

$CuInSe_2$ (CIS) and $CuGaSe_2$ (CGS), compound semiconductors of elements from groups I, III and VI in the periodic table, are typical representatives of a broad class of substances with different properties, so-called chalcopyrite.[6] $CuInSe_2$ and $CuGaSe_2$ form $CuIn_xGa_{1-x}Se_2$ alloy (CIGS) in any ratio of components. Importantly, varying the ratio of $CuInSe_2$ and $CuGaSe_2$, there is a slight change in the material parameters except the band gap. The possibility of regulating the band gap semiconductor in the range of 1.0-1.04 eV for $CuInSe_2$ to 1.68 eV for $CuGaSe_2$ are doubtless advantages of $CuIn_xGa_{1-x}Se_2$ (Birkmire, 2008).[7] The dependence of the band gap of $CuIn_xGa_{1-x}Se_2$ on $x$ is described by the formula (Alonso, 2002):

$$E_g(x) = 1.010 + 0.626x - 0.167x(1-x)\,. \tag{2}$$

For a long time, $CuInSe_2$ and $CuIn_xGa_{1-x}Se_2$ have been considered as promising materials for high-performance thin-film solar cells and fabrication of monolithically interconnected modules intended for cost-effective power generation (Shafarman & Stolt, 2003).
Parameters of $CuIn_xGa_{1-x}Se_2$ can be fitted as optimal for the photoelectric conversion. The fundamental absorption edge is well described by expression $a \sim (h\nu - E_g)^{1/2}/h\nu$ as for a typical direct band gap semiconductor. When the photon energy $h\nu$ exceeds the band gap $E_g$, the absorption coefficient of material from any content of Ga quickly exceeds values ~ $10^4$ $cm^{-1}$ so that the absorptivity of the material turns out to be the largest among all thin film (Fig. 4). This ensures effective absorption of solar radiation by $CuIn_xGa_{1-x}Se_2$ layer of micron-level thick – an important factor in reducing the cost of production. Efficiency of $CuInSe_2$ solar cell is within 12-15%, and in the case of $CuIn_xGa_{1-x}Se_2$ a record value of ~ 20% is reached among all types of thin-film solar cells (Repins, et al., 2008; Green et al, 2011). Widening the band gap of $CuIn_xGa_{1-x}Se_2$ leads to an increase in open circuit voltage while reducing the absorptivity of the material and hence decreasing the short circuit current. Theoretical estimation shows that the maximum efficiency of solar cells should be observed when $E_g$ = 1.4-1.5 eV, when the atomic ratio for Ga in CIGS is ~ 0.7, but according to the experimental data, this occurs when $E_g \approx 1.15$ eV that corresponds to Ga/(Ga+In) ≈ 0.3.

[6] Chalcopyrite (copper pyrite) is a mineral $CuFeS_2$, which has a tetragonal crystal structure.
[7] Sometimes part of Se atoms substitute for S.

Structural, electrical and optical properties of $CuIn_xGa_{1-x}Se_2$ are sensitive to deviations from the stoichiometric composition, native defects and grain sizes in the film. Because of the native defects (mainly In vacancies and Cu atoms on In sites), the conductivity of CIGS is p-type. It can be controlled by varying the Cu/In ratio during growth of the material. Stoichiometric and copper-enriched material has a p-type conductivity and grain sizes of 1-2 μm, while the material indium-enriched has n-type conductivity and smaller grains. $CuIn_xGa_{1-x}Se_2$ within the solar cell contains a large amount of Na (~ 0.1%), which are predominantly found at the grain boundaries rather than in the bulk of the grains and can improve solar cell performance. Depending on the pressure of selenium, the type conductivity of material as a result of annealing can be converted from p-type to n-type – or vice versa. Charge carrier density can vary widely from $10^{14}$ $cm^{-3}$ to $10^{19}$ $cm^{-3}$. In general, the desirable conductivity and carrier concentration can be relatively easy to obtain without special doping, but only the manipulating technological conditions of $CuIn_xGa_{1-x}Se_2$ deposition.

Literature data on the charge carrier mobility in thin-film $CuIn_xGa_{1-x}Se_2$ are quite divergent. The highest hole mobility is fixed as 200 $cm^2/V{\cdot}s$ at $10^{17}$ $cm^{-3}$ hole concentration. It is likely that the conductivity across grain boundaries in this case plays a significant role. In $CuIn_xGa_{1-x}Se_2$ single crystals, mobility of holes lies within the 15-150 $cm^2/V{\cdot}s$ range for holes and in the 90-900 $cm^2/V{\cdot}s$ range for electrons (Neumann & Tomlinson, 1990; Schroeder & Rockett, 1997).

The first photovoltaic structures based on $CuInSe_2$ with efficiency of ~ 12% were established back in 1970's by evaporating n-CdS onto p-$CuInSe_2$ single crystal (Wagner et al., 1974; Shay et al., 1975). Shortly thin-film CdS/$CuInSe_2$ solar cells were fabricated with efficiency 4-5% (Kazmerski et al., 1976), interest to which became stable after the Boeing company had reached 9.4% efficiency in 1981 (Mickelson & Chen, 1981; Shafarman & Stolt, 2003). Such solar cells were produced by simultaneous thermal evaporation of Cu, In and Se from separate sources on heated ceramic substrates coated with thin layer of Mo (*thermal multi-source co-evaporation process*). Later the method of simultaneous deposition Cu, In, Ga and Se become widely used to create $CuIn_xGa_{1-x}Se_2$ layers. Chemical composition of material is determined by temperatures of sources: 1300-1400° C for Cu, 1000-1100°C for In, 1150-1250°C for Ga and 300-350°C for Se. The main advantage of this technology is its flexibility; the main problem is the need for careful control of flow of Cu, In, Ga and Se, without which it is impossible to have adequate reproducibility characteristics of the film. In this regard, attractive is the so-called *two-step process*, that is, the deposition of Cu, In and Ga on substrates at a low temperature with subsequent a reactive heat-treatment of Cu-In-Ga films in a hydrogen-selenium ($H_2Se$) atmosphere at temperatures above ~ 630°C (Chu et al., 1984). Application of Cu, In and Ga can be achieved by various methods at low temperatures, among them is ion sputtering, electrochemical deposition and other methods that are easier to implement in mass production. Selenization can be conducted at atmospheric pressure at relatively low temperatures of 400-500°C. The main problem of this technology is the complexity of controlling the chemical composition of material as well as high toxicity of $H_2Se$.

To date, the co-deposition of copper, indium, gallium and selenium as well as selenization remain the main methods in the manufacture of CIGS solar cells.

In the first thin-film $CuInSe_2$ solar cells, heterojunction was made by deposition of CdS on $CuInSe_2$ thin film, which also served as front transparent electrode (Mickelson & Chen, 1981). Characteristics of solar cell are improved if on $CuInSe_2$ (or $CuIn_xGa_{1-x}Se_2$) first to

deposit undoped CdS, and then low-resistive CdS doped with In or Ga (pre-inflicted undoped CdS layer is called the "buffer" layer). Due to a relatively narrow band gap (2.42 eV), CdS absorbs solar radiation with a wavelengths $\lambda < 520$ nm, without giving any contribution to the photovoltaic efficiency. Absorption losses in the CdS layer can be reduced by increasing the band gap, alloying with ZnS (CdZnS) that results in some increase in the efficiency of the device. Its further increase is achieved by thinning CdS layer to 50 nm or even 30 nm followed by deposition of conductive ZnO layer, which is much more transparent in the whole spectral region (Jordan, 1993; Nakada, T. & Mise, 2001). The best results are achieved when ZnO is deposited in two steps, first a high-resistance ZnO layer and then a doped high-conductivity ZnO layer. Often, ZnO films are deposited by magnetron sputtering from ZnO:$Al_2O_3$ targets or by reactive sputtering, which requires special precision control technology regime. For high-efficiency cells the TCO deposition temperature should be lower than 150°C in order to avoid the detrimental interdiffusion across CdS/CIGS interface (Romeo et al., 2004).

Usually, Cu(In,Ga)$Se_2$ solar cells are grown in a substrate configuration which provides favorable process conditions and material compatibility. Structure of a typical solar cell is shown in Fig. 9. To reduce the reflection losses at the front surface of ZnO, an anti-refection $MgF_2$ coating with thickness of ~ 100 nm is also practised. The substrate configuration of solar cell requires an additional encapsulation layer and/or glass to protect the cell surface. In modules with cover glasses, to use any anti-refection coating is not practical.

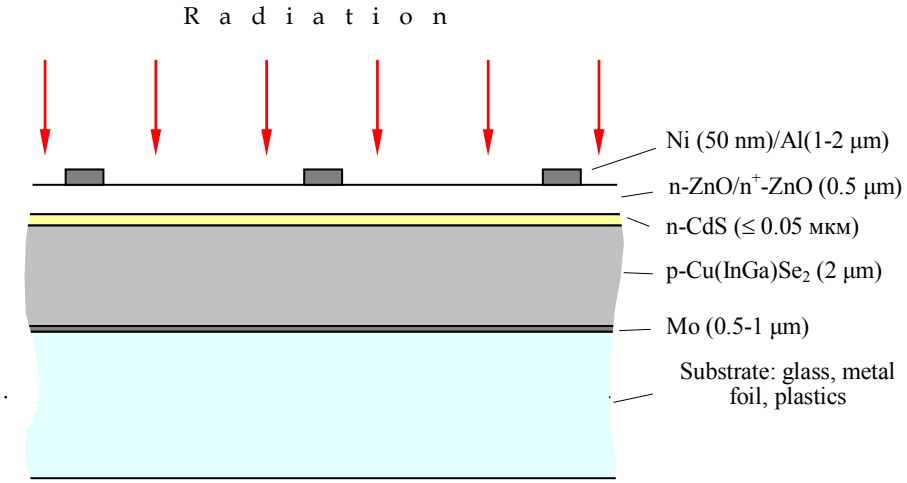


Fig. 9. Schematic cross section of a typical Cu(In,Ga)$Se_2$ solar module.

CdS layer is made by chemical precipitation from an aqueous alkali salt solution of cadmium ($CdCl_2$, $CdSO_4$, CdI2, $Cd(CH3COO)_2$), ammonia ($NH_3$) and thiourea $Sc(NH_2)_2$ in molar ratio, for example, 1.4:1:0.1 (*chemical bath deposition*). Pseudo-epitaxial deposition of CdS dense films is carried out by immersing the sample in electrolyte for several minutes at temperatures from 60 to 80°C or at room temperature followed by heating electrolyte to the same temperature. The pseudo-epitaxial character of deposition is promoted, firstly, by small (~ 0.6%) difference of $CuInSe_2$ and CdS lattice spacing, which, however, increases with

increasing Ga content in $CuInxGa_{1-x}Se_2$ (to ~ 2% at $x$ = Ga/(Ga+In) = 0.5), and, secondly, by the cleansing effect of electrolyte as a surface etchant of $CuIn_xGa_{1-x}Se_2$ (ammonia removes oxides on the surface). Depending on the conditions of deposition, the film may have hexagonal, cubic or a mixed structure with crystallite sizes of several tens of nanometers. Typically, film is somewhat non-stoichiometric composition (with an excess of Cd) and contains impurities O, H, C, N that can become apparent in a noticeable narrowing of the band gap. It is believed that the Cd in $Cu(InGa)Se_2$ modules can be handled safely, both with respect to environmental concerns and hazards during manufacturing (Shafarman & Stolt, 2003).

At relatively low temperature of deposition, the mutual penetration (migration) of elements at the $CdS/CuIn_xGa_{1-x}Se_2$ interface takes place to a depth of 10 nm (Cd replace Cu). It should be noted that vacuum deposition of CdS, used in solar cells on single crystals $CuIn_xGa_{1-x}Se_2$, is not suitable for thin film structures and does not allow to obtain the dense film of necessary small thickness and requires too high deposition temperature (150-200ºC). Deposition of CdS by ion sputtering gives better results, but still inferior to chemical vapor deposition.

Metal contacts in the form of narrow strips to the front surface of $Cu(In,Ga)Se_2$ device is made in two steps: first a thin layer of Ni (several tens of nanometers), and then Al layer with thickness of several microns. Purpose of a thin layer is to prevent the formation of oxidation layer.

As substrate for $CuIn_xGa_{1-x}Se_2$ solar cells, the window soda-lime-silica glass containing 13-14% $Na_2O$ can be used. The coefficients of linear expansion of this glass and $CuIn_xGa_{1-x}Se_2$ are quite close ($9\times10^{-6}$ $K^{-1}$) in contrast to borosilicate glass, for which the coefficient of linear expansion is about half. Glass is the most commonly used substrate, but significant efforts have been made to develop flexible solar cells on polyimide and metal foils providing less weight and flexible solar modules. Highest efficiencies of 12.8% and 17.6% have been reported on polyimide and metal foils, respectively (Tiwari etal., 1999; Tuttle et al., 2000). $Cu(In,Ga)Se_2$ modules have shown stable performance for prolonged operation in field tests.

As already mentioned, it is believed that the p-n junction is formed between p-$CuIn_xGa_{1-x}Se_2$ and n-ZnO, "ideal" material that serves as a "window" of solar cell (ZnO has band gap of 3.2 eV, high electrical conductivity and thermal stability). However, a thin underlayer CdS (~ 0.05 nm) affect a strong influence on the characteristics of solar cell by controlling the density of states at the interface and preventing unwanted diffusion of Cu, In, Se in ZnO.

Somewhat simplified energy diagram of solar cell based on $CuIn_xGa_{1-x}Se_2$ is shown in Fig. 10.

Band discontinuity $\Delta E_c$ = 0.3 eV at the $CdS/CuIn_xGa_{1-x}Se_2$ interface causes considerable band bending near the $CuIn_xGa_{1-x}Se_2$ surface, and, thus, the formation of p-n junction (Schmid et al., 1993). Diffusion of Cd in $CuIn_xGa_{1-x}Se_2$ during chemical vapor deposition of CdS also promotes this resulting in forming p-n *homojunction near surface* of $CuIn_xGa_{1-x}Se_2$.

Marginal impact of losses caused by recombination at the $CdS/CuIn_xGa_{1-x}Se_2$ interface is explained by the creation of p-n junction, despite the fact that no measures are preventable to level the lattice difference and defects on the surface which is in the air before deposition of CdS.

As always, the short-circuit current of $CuIn_xGa_{1-x}Se_2$ solar cell is the integral of the product of the external quantum efficiency and the spectral density of solar radiation power. $QE_{ext}$, which, in turn, is determined primarily by the processes of photoelectric conversion in the $CuIn_xGa_{1-x}Se_2$ absorber layer, i.e. by the internal quantum yield of the device $QE_{int}$.

It is believed that the solar cell can neglect recombination losses at the $CdS/Cu(In,Ga)Se_2$ interface and in the space-charge region and then one can write (Fahrenbruch A. & Bube, 1983):

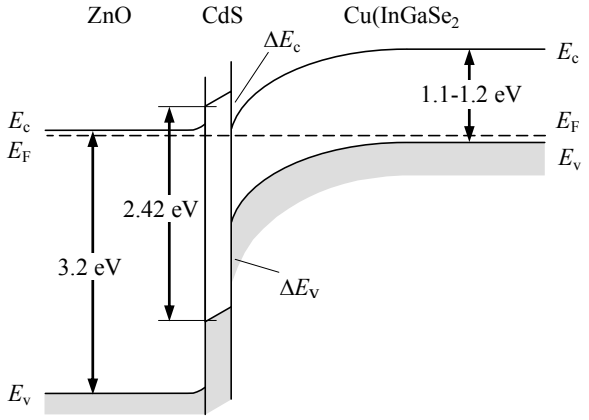


Fig. 10. Energy diagram of ZnO/CdS/$CuIn_xGa_{1-x}Se_2$ solar cell.

$$QE_{\text{int}} = 1 - \frac{\exp(-\alpha W)}{1 + \alpha L_n}, \tag{3}$$

where $a$ is the light absorption coefficient, and $W$ is the space-charge region width.

Besides $QE_{\text{int}}$, external quantum efficiency is also controlled by the above-mentioned reflection at the front surface of the device, reflection at all other interfaces, the band gap of $CuIn_xGa_{1-x}Se_2$ and the transmittances of CdS and ZnO window layers.

Fig. 11 shows the measured spectral distribution of quantum efficiency of solar cells based on $CuIn_xGa_{1-x}Se_2$ with different composition $x$ = 0, 0.24 and 0.61, and hence with different band gap of semiconductor $E_g$ = 1.02, 1.16 and 1.40 eV, respectively.

Another important characteristic of $CuIn_xGa_{1-x}Se_2$ solar cell, the open-circuit voltage, is determined by the charge transport mechanism in the heterostructure. Neglecting recombination at the interface of CdS-$CuIn_xGa_{1-x}Se_2$, the current-voltage characteristics of solar cells can be presented in the form

$$J = J_d - J_{ph} = J_o \exp\left[\frac{q}{nkT}(V - R_s J)\right] + GV - J_{ph} \tag{4}$$

where $J_d$ is the dark current density, $J_{ph}$ is the photocurrent density, $n$ is the ideality factor, $R_s$ is the series resistance, and $G$ is the shunt conductivity.

The experimental curves are often described by Eq. (4) at $n$ = 1.5 ± 0.3 that leads to the conclusion that the dominant charge transfer mechanism is recombination in the space charge region. If recombination level is located near mid-gap, $n \approx 2$, and in case of shallow level $n \approx 1$. In real $CuIn_xGa_{1-x}Se_2$, the levels in the band gap are distributed quasi-continuously.

If the minority carrier diffusion length is short, the losses caused by recombination at the rear surface of $CuIn_xGa_{1-x}Se_2$ is also excluded. In the best solar cells the electron lifetime is $10^{-8}$-$10^{-7}$ s (Nishitani et al., 1997; Ohnesorge et al., 1998). When describing transport properties $CuIn_xGa_{1-x}Se_2$, it can to be acceptable that grain boundaries do not play any noticeable role since the absorber layer has a *columnar structure* and the measured current does not cross the grain boundaries. As notes, solar cells have the highest photovoltaic efficiency if $x$ = Ga/(In + Ga) ≈ 0.3, i.e., $E_g \approx 1.15$ eV. Under AM1.5 global radiation, the

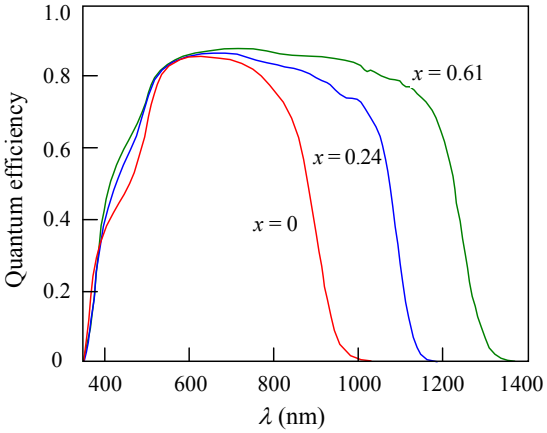


Fig. 11. Spectral distribution of quantum efficiency of $CuIn_xGa_{1-x}Se_2$ solar cells with x = 0, 0.24 and 0.61 (Shafarman & Stolt, 2003).

highest value of short-circuit current density $J_{sc}$ = 35.2 mA/sm² is observed for solar cells with $E_g$ = 1.12 eV (Contreras et al., 1999). If short-circuit current decreases with increasing Ga content, the open-circuit voltage $V_{oc}$ increases. With increasing temperature $V_{oc}$ markedly reduces. For $E_g$ = 1.16 eV, for example, $V_{oc}$ reduces from ~ 0.75 V at 220 K to ~ 0.55 V at 320 K. Introduction of Ga in $CuInSe_2$ compound attracts of professionals by the fact that it reduces the cost of In, which is widely used in LCD monitors, computers, TV screens and mobile phones. Therefore there is an attempt to reduce the content of In in $CuIn_xGa_{1-x}Se_2$ solar cells up to 5-10%, even slightly losing the photovoltaic conversion efficiency.

The efficiencies of laboratory $CuIn_xGa_{1-x}Se_2$ solar cells and modules of large area are significantly different. The reason is that the production of modules requires the introduction of technology different qualitatively from that used in the traditional semiconductor electronics, and a significant lack of deep scientific basis of applied materials. As a result of research, aimed to reducing the cost of $CuIn_xGa_{1-x}Se_2$ solar modules (which were originally more expensive compared to devices on amorphous silicon), Würth Solar (Germany) and Shell Solar Industries (USA) developed the first commercial $CuIn_xGa_{1-x}Se_2$ solar modules and initiated their large-scale production, which began in 2006 in Germany.

In the production of such modules are also engaged other companies in a number of countries, among them Zentrum für Sonnenenergie- und Wasserstoff-Forschung – ZSW (Germany), Energy Photovoltaics, Inc. and International Solar Electric Technology (USA), Angstrom Solar Centre (Sweden), Showa Shell and Matsushita (Japan) and others. Technology for production of solar modules on flexible substrates involving «roll-to-roll» technology was developed by Global Solar Energy (USA, Germany).

$CuIn_xGa_{1-x}Se_2$-based photovoltaics, along with other thin-film PV devices, continue to attract an interest first and foremost because of their potential to be manufactured at a lower cost than Si wafer or ribbon based modules. To reach their potential for large-scale power generation with higher throughput, yield, and performance of products, there is a need for continued improvement in the fundamental science, deposition equipment and processes based on well-developed models. Note also that the scarce supply of In may make it difficult to implement CIGS technology on a large scale.

### 3.3 Cadmium telluride

Cadmium telluride (CdTe) is a semiconductor with the band gap of 1.47-1.48 eV (290-300 K), optimal for solar cells. As a-Si, CIS and CIGS, CdTe is a direct-gap semiconductor, so that the thickness of only a few microns is sufficient for almost complete absorption of solar radiation (97-98%) with photon energy $h\nu > E_g$ (Fig. 4). As the temperature increases the efficiency of CdTe solar cell is reduced less than with silicon devices, which is important, given the work of solar modules in high-power irradiation. Compared to other thin-film materials, technology of CdTe solar modules is simpler and more suitable for large-scale production.

Solar cells based on CdTe have a rather long history. Back in 1956, Loferski theoretically grounded the use of InP, GaAs and CdTe in solar cells as semiconductors with a higher efficiency of photoelectric conversion compared with CdS, Se, AlSb and Si (Loferski, 1956). However, the efficiency of laboratory samples of solar cells with p-n junctions in monocrystalline CdTe, was only ~ 2% in 1959, has exceeded 7% only in 20 years and about 10% later (Minilya-Arroyo et al, 1979; Cohen-Solal et al., 1982). The reason for low efficiency of these devices were great losses caused by surface recombination and technological difficulties of p-n junction formation with a thin front layer. Therefore, further efforts were aimed at finding suitable *heterostructures*, the first of which was p-$Cu_2Te$/n-CdTe junction with efficiency of about 7%, that was proved too unstable through the diffusion of copper. It was investigated other materials used as heteropartners of n-type conductivity with wider band gap compared with CdTe: ITO, $In_2O_3$, ZnO performed the function of "window" through which light is introduced in the photovoltaic active layer of absorbing CdTe.

In 1964, the first heterojunctions obtained by spraying a thin layer of n-CdS on the surface of p-CdTe single crystal were described (Muller & Zuleeg, 1964). The first *thin-film* CdTe/CdS/$SnO_2$/glass structures that became the prototype of modern solar cells, was established in Physical-Technical Institute, Tashkent, Uzbekistan in 1969 (Adirovich et al., 1969). Over the years it became clear that the CdS/CdTe heterostucture has a real prospect of the introduction into mass production of solar modules, despite the relatively narrow band gap of CdS as a "window" layer. The crystal of CdTe adopts the wurtzite crystal structure, but in most deposited CdTe films, hexagonally packed alternating Cd and Te layers tend to lie in the plane of the substrate, leading to columnar growth of crystallites. At high temperature, CdTe grows stoichiometrically in thin-film form as natively p-doped semiconductor; no additional doping has to be introduced. Nevertheless, the cells are typically “activated” by using the influence of $CdCl_2$ at elevated temperatures (~ 400°C) that improves the crystallinity of the material.

In the early 21st century it has been succeeded to achieve a compromise between the two main criteria acceptable for manufacturing CdTe solar modules – sufficient photoelectric conversion efficiency and cheapness of production (Bonnet, 2003). This was possible thanks to the development of a number of relatively simple and properly controlled method of applying large area of CdTe and CdS thin layers that is easy to implement in large-scale production: close-space sublimation, vapor transport deposition, electrodeposition, chemical bath deposition, sputter deposition, screen printing. Obstruction caused by considerable differences of crystal lattice parameters of CdTe and CdS (~ 5%), largely overcome by straightforward thermal treatment of the produced CdTe/CdS structure. It is believed that this is accompanied by a mutual substitution of S and Te atoms and formation an intermediate $CdTe_{1-x}S_x$ layer with reduced density of states at the interface of CdTe and CdS, which may adversely affect the efficiency of solar cell. Simple methods of production and

formation of barrier structures, that do not require complex and expensive equipment, are an important advantage of the solar cell technology based on CdTe.

When producing solar cells, CdS and CdTe layers are usually applied on a soda-lime glass superstrate (~ 3 mm thick), covered with a transparent electrically conductive oxide layer (TCO), e.g., F-doped $SnO_2$ ($SnO_2$:F) or ITO ($In_2O_3$ + $SnO_2$) (Fig. 12) (Bonnet, 2003).[8] They are often used in combination with a thin (high-resistivity) $SnO_x$ sublayer between the TCO and the CdS window layer, which prevents possible shunts through pinholes in the CdS and facilitates the use of a thinner CdS layer for reducing photon absorption losses for wavelengths shorter than 500 nm (Bonnet, 2002). At the final stage, after deposition of the back electrodes, solar cells are covered by another glass using the sealing material (etylenvinil acetate, EVA), which provides durability and stability of the devices within 25-35 years.

Processes of photoelectric conversion in thin-film CdS/CdTe structure are amenable to *mathematical description*. This is of practical importance because it allows to investigate the dependence of the efficiency of solar cells on the parameters of the materials and the barrier structure as well as to formulate recommendations for the technology. These parameters are, primarily, (i) the width of the space-charge region, (ii) the lifetime of minority carriers, (iii) their diffusion length, (iv) the recombination velocity at the front and back surfaces of the CdTe absorber layer, (v) its thickness.

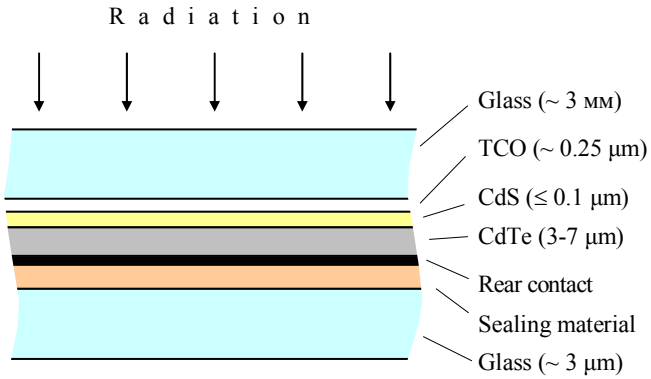


Fig. 12. Cross-section of thin film solar cell CdS/CdTe.

One of the main characteristics of a solar cell is the *spectral distribution of quantum efficiency* (spectral response), which is ultimately determined the short-circuit current density of the CdS/CdTe heterostructure.

It is known that in CdS/CdTe solar cells only the CdTe layer contributes to the light-to-electric energy conversion, while the CdS "window" layer only absorbs light in the range $\lambda$ < 500-520 nm thereby reducing the photocurrent. Therefore in numerous papers a band bending (and hence a depletion layer) in CdS is not depicted on the energy diagram (see, for example, Birkmire & Eser, 1997; Fritsche et al., 2001; Goetzberger et al, 2003), i.e. the

[8] The CdTe solar cells can be produced in both substrate and superstrate configurations, but the latter is preferable. The substrate can be a low-cost soda-lime glass for growth process temperatures below 550°C, or alkali-free glass for high-temperature processes (550–600°C) (Romeo et al., 2004).

depletion layer of the CdS/CdTe diode structure is virtually located in the p-CdTe layer (Fig. 13). This is identical to the case of an asymmetric abrupt p-n junction or a Schottky diode, i.e. the potential energy $\varphi(x,V)$ and the space-charge region width $W$ in the CdS/CdTe heterojunction can be expressed as (Sze, 1981):

$$\varphi(x,V) = (\varphi_o - qV)\left(1 - \frac{x}{W}\right)^2, \tag{5}$$

$$W = \sqrt{\frac{2\varepsilon\varepsilon_o(\varphi_o - qV)}{q^2(N_a - N_d)}}, \tag{6}$$

where $\varepsilon_o$ is the electric constant, $\varepsilon$ is the relative dielectric constant of the semiconductor, $\varphi_o = qV_{bi}$ is the barrier height at the semiconductor side ($V_{bi}$ is the built-in potential), $V$ is the applied voltage, and $N_a - N_d$ is the uncompensated acceptor concentration in the CdTe layer. The *internal* photoelectric quantum efficiency $\eta_{int}$ can be found from the continuity equation with the boundary conditions. The exact solution of this equation taking into account the *drift* and *diffusion components* as well as surface recombination at the interfaces leads to rather cumbersome and non-visual expressions (Lavagna et al., 1977). However, in view of the real CdS/CdTe thin-film structure, the expression for the *drift* component of the quantum efficiency can be significantly simplified (Kosyachenko et al., 2009):

$$\eta_{drift} = \frac{1 + \frac{S}{D_n}\left(\alpha + \frac{2}{W}\frac{\varphi_o - qV}{kT}\right)^{-1}}{1 + \frac{S}{D_n}\left(\frac{2}{W}\frac{\varphi_o - qV}{kT}\right)^{-1}} - \exp(-\alpha W) \cdot \tag{7}$$

where $S$ is the recombination velocity at the front surface, $D_n$ is the electron diffusion coefficient related to the electron mobility $\mu_n$ through the Einstein relation: $qD_n/kT = \mu_n$.
For the *diffusion* component of the photoelectric quantum yield that takes into account surface recombination at the back surface of the CdTe layer, one can use the exact expression obtained for the p-layer in a p-n junction solar cell (Sze, 1981)

$$\eta_{dif} = \frac{\alpha L_n}{\alpha^2 L_n^2 - 1}\exp(-\alpha W) \times$$
$$\times\left\{\alpha L_n - \frac{\frac{S_b L_n}{D_n}\left[\cosh\left(\frac{d-W}{L_n}\right) - \exp(-\alpha(d-W))\right] + \sinh\left(\frac{d-W}{L_n}\right) + \alpha L_n \exp(-\alpha(d-W))}{\frac{S_b L_n}{D_n}\sinh\left(\frac{d-W}{L_n}\right) + \cosh\left(\frac{d-W}{L_n}\right)}\right\}, \tag{8}$$

where $d$ is the thickness of the CdTe absorber layer, $S_b$ is the recombination velocity at its back surface.
The *total* quantum yield of photoelectric conversion in the CdTe absorber layer is the sum of the two components: $\eta_{int} = \eta_{drift} + \eta_{dif}$.
Fig. 14 illustrates a comparison of the calculated curve $\eta_{ext}(\lambda)$ using Eqs. (5)-(8) with the measured spectrum (Kosyachenko et al., 2009). As seen, very good agreement between the calculated curve and the experimental points has been obtained.

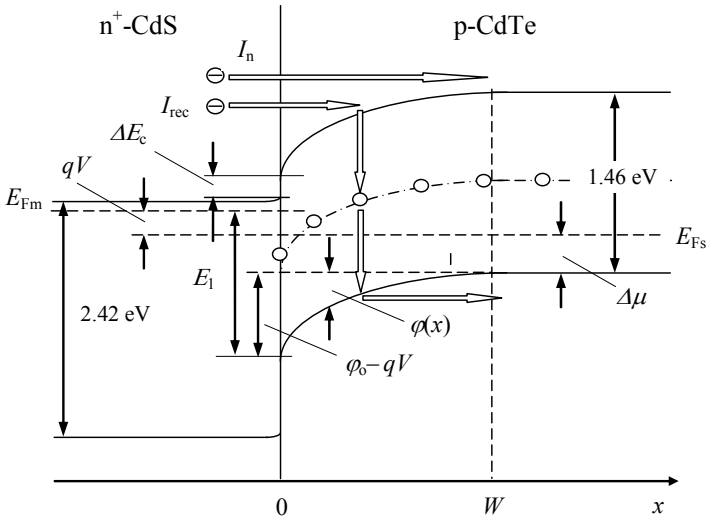


Fig. 13. The energy band diagram of CdS/CdTe thin-film heterojunction under forward bias. The electron transitions corresponding to the recombination current $I_{rec}$ and over-barrier diffusion current $I_n$ are shown.

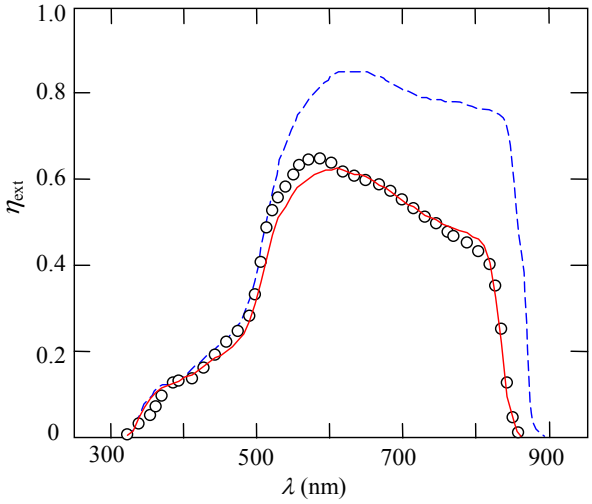


Fig. 14. Comparison of the measured (circles) and calculated (solid line) quantum efficiency spectrum $\eta_{ext}$. The dashed line shows the spectrum of 100 % *internal* efficiency.

The expressions for quantum efficiency spectra can be used to calculate the short-circuit current density $J_{sc}$ using AM1.5 solar radiation Tables ISO 9845-1:1992 (Standard ISO, 1992). If $\Phi_i$ is the spectral radiation power density and $h\nu$ is the photon energy, the spectral density of the incident photon flux is $\Phi_i/h\nu_i$ and then

$$J_{sc} = q\sum_i \eta_{\text{int}}(\lambda)\frac{\Phi_i(\lambda)}{h\nu_i}\Delta\lambda_i\,, \tag{9}$$

where $\Delta\lambda_i$ is the wavelength range between the neighboring values of $\lambda_i$ (the photon energy $h\nu_i$) in the table and the summation is over the spectral range 300 nm $\le \lambda \le \lambda_g = hc/E_g$.

The calculation results of the *drift* component of short-circuit current density $J_{\text{drift}}$ using Eqs. (7) and (9) lead to important practical conclusions (Kosyachenko et al., 2008).

If $S = 0$, the short-circuit current gradually increases with widening $W$ and approaches a maximum value $J_{\text{drift}} = 28.7$ mA/cm$^2$ at $W > 10$ μm. Surface recombination decreases $J_{\text{drift}}$ only in the case if the electric field in the space-charge region is not strong enough, i.e. when the uncompensated acceptor concentration $N_a - N_d$ is low. As $N_a - N_d$ increases and consequently the electric field strength becomes stronger, the influence of surface recombination becomes weaker, and at $N_a - N_d \ge 10^{16}$ cm$^{-3}$ the effect of surface recombination is virtually eliminated. However in this case, $J_{\text{drift}}$ decreases with increasing $N_a - N_d$ because a significant portion of radiation is absorbed outside the space-charge region. Thus, the dependence of drift component of the short-circuit current on the uncompensated acceptor concentration $N_a - N_d$ is represented by a curve with a maximum at $N_a - N_d \approx 10^{15}$ cm$^{-3}$ ($W \approx 1$ μm).

The *diffusion* component of short-circuit current density $J_{\text{dif}}$ is determined by the thickness of the absorber layer $d$, the electron lifetime $\tau_n$ and the recombination velocity at the back surface of the CdTe layer $S_b$. If, for example, $\tau_n = 10^{-6}$ s and $S_b = 0$, then the total charge collection in the neutral part is observed at $d$ = 15-20 μm and to reach the total charge collection in the case $S_b = 10^7$ cm/s, the CdTe thickness should be 50 μm or larger (Kosyachenko et al., 2008). In this regard the question arises why for total charge collection the thickness of the CdTe absorber layer $d$ should amount to several tens of micrometers. The matter is that, as already noted, the value of $d$ is commonly considered to be in excess of the effective penetration depth of the radiation into the CdTe absorber layer in the intrinsic absorption region of the semiconductor, i.e. in excess of $d = 10^{-4}$ cm = 1 μm. With this reasoning, the absorber layer thickness is usually chosen at a few microns. However, one does not take into account that the carriers, arisen outside the space-charge region, *diffuse* into the neutral part of the CdTe layer penetrating deeper into the material. Having reached the back surface of the CdTe layer, carriers recombine and do not contribute to the photocurrent. Considering the spatial distribution of photogenerated electrons in the neutral region shows that at $S_b = 7\times10^7$ cm/s, typical values of $\tau_n = 10^{-9}$ s and $N_a - N_d = 10^{16}$ cm$^{-3}$ and at $d$ = 1-2 μm, surface recombination "kills" most of electrons photogenerated in the neutral part of the CdTe layer (Kosyachenko et al., 2009).

Fig. 15 shows the calculation results of the *total* short-circuit current density $J_{sc}$ (the sum of the drift and diffusion components) vs. $N_a - N_d$ for different electron lifetimes $\tau_n$. Calculations have been carried out for the CdTe film thickness $d = 5$ μm which is often used in the fabrication of CdTe-based solar cells. As can be seen, at $\tau_n \ge 10^{-8}$ s the short-circuit current density is 26-27 mA/cm$^2$ when $N_a - N_d > 10^{16}$ cm$^{-3}$ and for shorter electron lifetime, $J_{sc}$ peaks at $N_a - N_d = (1\text{-}3)\times10^{15}$ cm$^{-3}$.

As $N_a - N_d$ is in excess of this concentration, the short-circuit current decreases since the drift component of the photocurrent reduces. In the range of $N_a - N_d < (1\text{-}3)\times10^{15}$ cm$^{-3}$, the short-circuit current density also decreases, but due to recombination at the front surface of the CdTe layer.

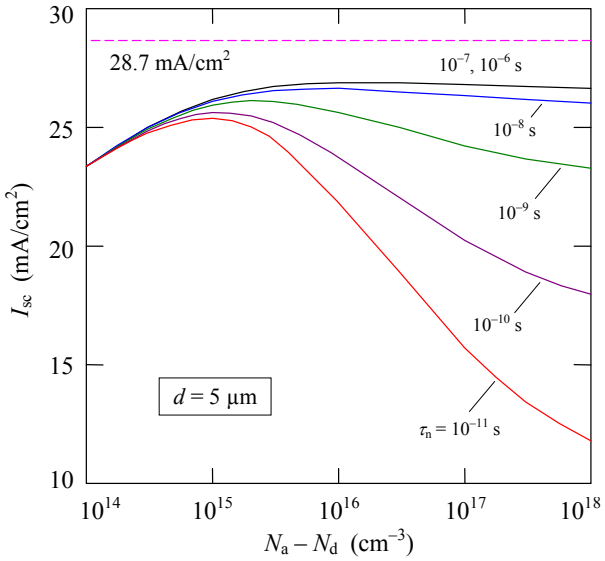


Fig. 15. *Total* short-circuit current density $J_{sc}$ of a CdTe-based solar cell as a function of the uncompensated acceptor concentration $N_a - N_d$ calculated at the absorber layer thickness $d$ = 5 μm for different electron lifetime $\tau_n$.

The *I-V* characteristic determined the open-circuit voltage and fill factor of CdS/CdTe solar cells is most commonly described by the semi-empirical formulae similar to Eq. (4), which consists the so-called "ideality" factor and is valid for some cases. Our measurements show, however, that such "generalization" of the formulae does not cover the observed variety of the CdS/CdTe solar cell *I-V* characteristics. The measured voltage dependences of the forward current are not always exponential and the saturation of the reverse current is *never* observed.

On the other hand, our measurements show that the *I-V* characteristics of CdS/CdTe heterostructures and their temperature variation are governed by the generation-recombination Sah-Noyce-Shockley theory (Sah at al., 1957). According to this theory, the dependence $I \sim \exp(qV/nkT)$ at $n \approx 2$ takes place only in the case, where the generation-recombination energy level is located near the middle of the band gap. If the level moves away from the mid-gap the coefficient $n$ becomes close to 1 but only at low forward voltage. If the forward voltage elevates, the *I-V* characteristic modifies in the dependence where $n \approx 2$ and at higher voltages the dependence $I$ on $V$ becomes even weaker (Sah et al., 1957; Kosyachenko et al., 2004). Certainly, at higher forward currents, it is also necessary to take into account the voltage drop across the series resistance $R_s$ of the bulk part of the CdTe layer by replacing the voltage $V$ in the discussed expressions with $V - I \cdot R_s$.

The Sah-Noyce-Shockley theory supposes that the generation-recombination rate in the space-charge region is determined by expression

$$U(x,V) = \frac{n(x,V)p(x,V) - n_i^2}{\tau_{po}\left[n(x,V) + n_1\right] + \tau_{no}\left[p(x,V) + p_1\right]}, \tag{10}$$

where $n(x,V)$ and $p(x,V)$ are the carrier concentrations in the conduction and valence bands, $n_i$ is the intrinsic carrier concentration. The $n_1$ and $p_1$ values in Eq. (10) are determined by the energy spacing between the top of the valence band and the generation-recombination level $E_t$, i.e. $p_1 = N_v \exp(-E_t/kT)$ and $n_1 = N_c \exp[-(E_g - E_t)/kT]$, where $N_c = 2(m_n kT/2\pi\hbar^2)^{3/2}$ and $N_v = 2(m_p kT/2\pi\hbar^2)^{3/2}$ are the effective density of states in the conduction and valence bands, $m_n$ and $m_p$ are the effective masses of electrons and holes, and $\tau_{no}$ and $\tau_{po}$ are the lifetime of electrons and holes in the depletion region, respectively.

The recombination current under forward bias and the generation current under reverse bias are found by integration of $U(x, V)$ throughout the entire depletion layer:

$$J_{gr} = q\int_0^W U(x,V)dx\,. \tag{11}$$

In Eq. (10) the expressions for $n(x,V)$ and $p(x,V)$ in the depletion region have the forms:

$$p(x,V) = N_c \exp\left[-\frac{\Delta\mu + \varphi(x,V)}{kT}\right], \tag{12}$$

$$n(x,V) = N_v exp\left[-\frac{E_g - \Delta\mu - \varphi(x,V) - qV}{kT}\right], \tag{13}$$

where $\Delta\mu$ is the energy spacing between the Fermi level and the top of the valence band in the bulk of the CdTe layer, $\varphi(x,V)$ is the potential energy given by Eq. (5).

Over-barrier (diffusion) carrier flow in the CdS/CdTe heterostructure is restricted by high barriers for both majority carriers (holes) and minority carriers (electrons) (Fig. 13). That is why, under low and moderate forward voltages, the dominant charge transport mechanism is caused by recombination in the space-charge region. However, as $qV$ nears $\varphi_o$, the over-barrier currents due to much stronger dependence on $V$ become comparable and even higher than the recombination current. Since in CdS/CdTe heterojunction the barrier for holes is considerably higher than that for electrons, the *electron* component dominates the over-barrier current, which can be written as (Sze, 1981):

$$J_n = q\frac{n_p L_n}{\tau_n}\left[\exp\left(\frac{qV}{kT}\right) - 1\right], \tag{14}$$

where $n_p = N_c \exp[-(E_g - \Delta\mu)/kT]$ is the concentration of electrons in the neutral part of the p-CdTe layer.

Thus, the dark current density $J_d(V)$ in CdS/CdTe heterostructure is the sum of the generation-recombination and diffusion components:

$$J_d(V) = J_{gr}(V) + J_n(V)\,. \tag{15}$$

The results of comparison between theory and experiment are demonstrated in Fig. 16 on the example of *I-V* characteristic, which reflects especially pronounced features of the transport mechanism in CdS/CdTe solar cell (Kosyachenko et al., 2010). As is seen, there is an extended portion of the curve ($0.1 < V < 0.8$ V), where the dependence $I \sim \exp(qV/AkT)$ holds for $n = 1.92$ (rather than 2!).

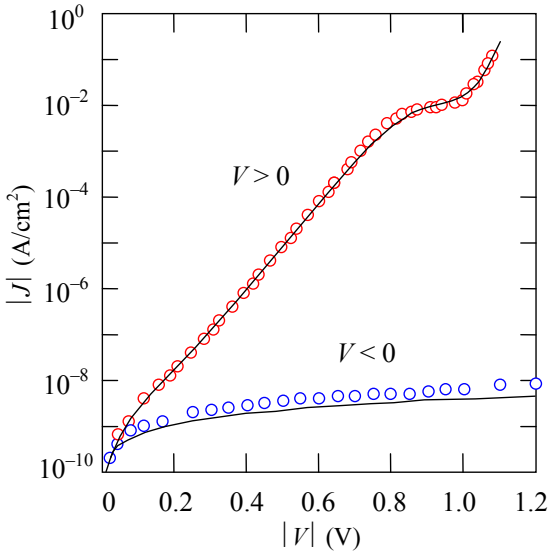


Fig. 16. Room-temperature *I-V* characteristic of thin-film CdS/CdTe heterostructure. The circles and solid lines show the experimental and calculated results, respectively.

At higher voltages, the deviation from the exponential dependence toward lower currents is observed. However, if the voltage elevates still further (> 1 V), a much steeper increase of forward current occurs. Analysis shows that all these features are explained in the frame of mechanism involving the generation-recombination in the space-charge region in a wide range of moderate voltages completed by the over-barrier diffusion current at higher voltages.

One can see in Fig. 16 that the *I-V* characteristic calculated in accordance with the above theory are in good agreement with experiment both for the forward and reverse connections of the solar cell. Note that the reverse current increases continuously with voltage rather than saturates, as requires the commonly used semi-empirical formula.

Knowing the dark *I-V* characteristic, one can find the *I-V* characteristic under illumination as

$$J(V) = J_d(V) - J_{ph} \tag{16}$$

and determine the open-circuit voltage and fill factor. In Eq.(16) $J_d(V)$ and $J_{ph}$ are the dark current and photocurrent densities, respectively. Of course, it must be specified a definite value of the density of short circuit current $J_{sc}$. Keeping in view the determination of conditions to maximize the photovoltaic efficiency, we use for this the data shown in Fig. 15, i.e. set $J_{sc} \approx 26$ mA/cm$^2$. This is the case for $N_a - N_d = 10^{15}$-$10^{16}$ cm$^{-3}$ and a film thickness $d = 5$ μm, which is often used in the fabrication of CdTe-based solar cells.

Fig. 17 shows the open-circuit voltage $V_{oc}$ and the efficiency $\eta$ of CdS/CdTe heterostructure as a function of effective carrier lifetime $\tau$ calculated for various resistivities of the p-CdTe layer $\rho$.

As seen in Fig. 17(a), the open-circuit voltage $V_{oc}$ considerably increases with lowering $\rho$ and increasing $\tau$ (as $\rho$ varies, $\Delta\mu$ also varies affecting the value of the recombination current, and especially the over-barrier current).

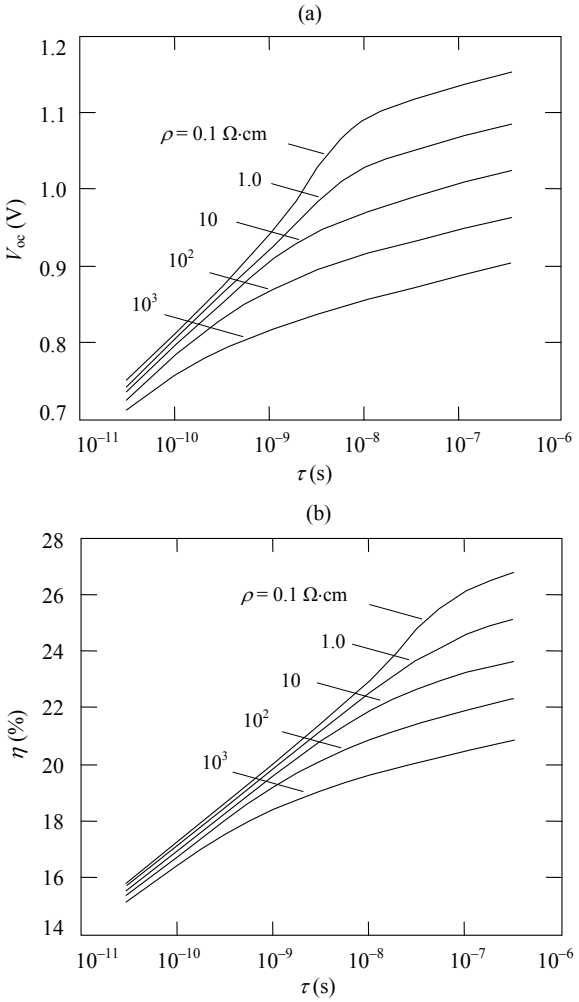


Fig. 17. Dependences of the open-circuit voltage $V_{oc}$ (a) and efficiency $\eta$ (b) of CdS/CdTe heterojunction on the carrier lifetime $\tau$ calculated by Eq. (16) using Eqs. (10)-(15) for various resistivities $\rho$ of the CdTe layer.

In the most commonly encountered case, as $\tau = 10^{-10}$-$10^{-9}$ s, the values of $V_{oc}$ = 0.8-0.85 V (0.75-0.8 V for commercial devices) are far from the maximum possible values of 1.15-1.2 V, which are reached on the curve for $\rho$ = 0.1 Ω·cm and $\tau > 10^{-8}$ s.

As seen in Fig. 17(b), the dependence of the efficiency $\eta = P_{out}/P_{irr}$ on $\tau$ remarkably increases from 15-16% to 21-27.5% when $\tau$ and $\rho$ changes within the indicated limits ($P_{irr}$ is the AM 1.5 solar radiation power 100 mW/cm$^2$). For $\tau = 10^{-10}$-$10^{-9}$ s, the efficiency lies near 17-19% and the enhancement of $\eta$ by lowering $\rho$ of the CdTe layer is 0.5-1.5%. Thus, assuming $\tau = 10^{-10}$-$10^{-9}$ s, the calculated results turn out to be quite close to the experimental efficiencies of the best thin-film CdS/CdTe solar cells (16-17%).

The enhancement of $\eta$ from 16-17% to 27-28% is possible if the carrier lifetime increases to $\tau \geq 10^{-6}$ s and the resistivity of CdTe reduces to $\rho \approx 0.1$ Ω·cm. This also requires an increase in the short-circuit current density. As follows from the foregoing, the latter is possible for the thickness of the CdTe absorber layer of 20-30 μm and even more. Evidently, this is not justified for large-scale production of solar modules.

In the early years of 21 century, the technology and manufacturing of solar modules based on CdTe, which could compete with silicon counterparts was developed. With mass production, the efficiency of CdTe modules is 10-11% with the prospect of an increase in a few percents in the coming years (Multi Year Program Plan, 2008). The cost of modules over the past five years has decreased three times and crossed the threshold $1.0 per Wp, that is much less than wafer or ribbon based modules on silicon. In 2012-2015, the cost of CdTe-based solar modules is expected to be below $ 0.7 per Wp.

It should be noted that the growth rates of CdTe module production over the last decade are the highest in the entire solar energy sector. Over the past 5 years, their annual capacity increased more than an order of magnitude, greatly surpassing the capacity of the counterparts based on a-Si and in a few times – based on CIS (CIGS). In Germany, Spain, USA and other countries, CdTe solar photovoltaic power plants with a capacity of several megawatts up to several tens of megawatts have been built. Annual production of solar modules based on CdTe by only one company First Solar, Inc. in 2009-2010 exceeded 1.2 GW). This company is the largest manufacturer of solar modules in the world, which far exceeded the capacities of perennial leaders in the manufacture of solar modules and continues to increase production, despite the economic and financial crisis. Other well known companies such as AVA Solar and Prime Star Solar (USA), Calyxo GmbH and Antec Solar Energy AG (Germany), Arendi SRL (Italy) are also involved in the production of CdTe solar modules. In May 2010 the General Electric company announced plans to introduce production of CdTe thin-film solar modules based on technology developed at the National Renewable Energy Laboratory and PrimeStar Solar. These facts remove any doubt on the prospects of solar energy based on CdTe.

One of the arguments advanced against the use of CdTe in solar energy is based on the fact that natural resources of Cd and Te are limited.

Indeed, Cd and Te are rare and scattered elements; their content in the earth's crust is ~ $10^{-5}$% and ~ $10^{-7}$-$10^{-6}$%, respectively. Currently, there are no commercial deposits of Cd and Te in the world; Cd and Te are extracted as byproducts in the production of mainly zinc and copper, respectively. The limiting raw factor for development of solar energy through the production of CdTe is Te. For the world needs, cadmium is annually produced just 150-200 tons. According to the National Renewable Energy Laboratory, the U.S. Department of Energy and other agencies, annual production of Te as a byproduct of copper production can be increased to ~ 1.5 tons. For the module production with capacity of 1 GW, approximately 70 tons of Te are needed at present 10-11% efficiency of modules. Using each year, for example, 1 thousand tons one can make solar modules with power ~ 15 GW. Thus, through Te only as a byproduct in the production of Cu, accelerated development of solar energy based on CdTe can last for several decades. Other currently unused stocks of tellurium, particularly in South America, China, Mexico and other places of the globe are also known. With good reason Te was not the focus of geological exploration, however, studies in recent years show that, for example, underwater crusts throughout the ocean basins is extremely rich in Te, whose content of Te ~ $10^9$ times higher compared with ocean water and ~ $10^4$ times higher than in the Earth's crust (Hein et al., 2003). These stocks of

tellurium in a relatively small depth of ocean (e.g. ~ 400 m) can easily meet the needs of the whole world's energy. It should also be noted that the additional costs of Cd and Te will not arise after 25-35 years, when CdTe solar panels expend their resources. The technologies for *recycling* the worked-out products, which allows majority of the components (~ 90%) to use in the production of new solar modules, have been already developed.

Another objection to the proliferation of CdTe solar cells, which opponents argue, is that the Cd, Te and their compounds are extremely harmful to humans.

Indeed, Cd and Te are toxic heavy metals; Cd is even cancer-causing element. However, the research of many independent experts of the National Renewable Energy Laboratory and Brookhaven National Laboratory show that CdTe compound is chemically stable, biologically inert and does not constitute a threat to human health and the environment both in terms of production and exploitation of solar modules (Bonnet, 2000; Fthenakis, 2008). Cd emissions to the atmosphere is possible only if the temperature exceeds ~ 1050ºC in case of fire. However, CdTe in solar module is between two glass plates in a sealed condition. With this design, glass will melt at temperatures much lower than 1050ºC, CdTe will turn in the molten mass that does not allow the allocation of Cd and Te in the atmosphere. It has been shown that the release of cadmium to the atmosphere is lower with CdTe-based solar cells than with silicon photovoltaics. Despite much discussion of the toxicity of CdTe-based solar cells, this is technology that is reliably delivered on a large scale.

## 4. Conclusions

Analysis of photovoltaics development leads to the negative conclusion that the desired rate of increase in the capacity of solar energy based on single-crystalline, polycrystalline and amorphous silicon can not be provided. Despite a long history, the share of PV currently amounts to a small fraction of the overall balance of the world power sector, and even according to the most optimistic forecasts, will not dominate in 2050. Resources of hydroelectric and wind energy are limited, the expansion of nuclear power is highly problematic from a security standpoint. This means that a significant fraction of the energy will be generated by natural gas, oil, coal, oil shale, biomass, which can lead to irreversible changes in climate on Earth. The main reason for the slow development of the photovoltaics based on wafer or ribbon silicon (as its main direction) is the high consumption of materials, energy and labor, and hence too low productivity and high cost of production. This is determined by the *fundamental* factor because the single-crystalline and polycrystalline silicon are indirect-gap semiconductors. The technology of solar modules based on direct-gap amorphous silicon is quite complicated, and their stabilized efficiency is too low for use in large-scale energy. In this regard, there is an urgent need to involve other areas of photovoltaics in energy production. Thin-film technologies using direct-gap semiconductors such as CIGS and CdTe hold the promise of significantly accelerating the development of photovoltaics. Intensive research and development of thin-film technologies based on other materials, for example, organic and die-sensitizes solar cells is also being conducted. The main advantages of thin-film technology are less material consumption, lower requirements to the parameters of the materials, ease of engineering methods of manufacture, and the possibility of full automation. All of this provides better throughput of manufacturing and lower production costs, i.e. just what is lacking in wafer or ribbon based silicon photovoltaics. CdTe and CIGS based modules have proved their viability. Solar power stations based on these materials with a capacity from a few megawatts to a few tens of megawatts have already

been built; several agreements for the construction of such plants with a capacity higher by one or even two orders of magnitude have been concluded. A growing number of companies are involved in the production of CdTe and CIGS based modules. Broad front of research on the possibility of increasing the efficiency of the modules, which in mass production is much lower than the theoretical predictions, are being conducted. The aforesaid, of course, does not preclude participation in the production of electrical energy of photovoltaics based on single-crystalline, polycrystalline, ribbon and amorphous silicon with different designs of solar cell structures. A large number of companies are involved in the production of the silicon modules, which are continually evolving, making a potential contribution to the energy, but they cannot solve the problem globally for the foreseeable future.

## 5. Acknowledgements

I thank X. Mathew, Centro de Investigacion en Energia-UNAM, Mexico, for the CdS/CdTe thin-film heterostructures, V.M. Sklyarchuk for sample preparation to study, E.V. Grushko for measurements and all participants of the investigation for helpful discussion. The study was supported by the State Foundation for Fundamental Investigations of Ukraine within the Agreements Φ14/259-2007 and Φ40.7/014.

## 6. References

Adirovich, E.I., Yuabov, Yu.M., Yagudaev, G.R. (1969). Photoelectric phenomena in film diodes with heterojunction. *Sov. Phys. Semicond*. 3, 61-65

Alonso, M.I., Garriga, M., Durante Rincón, C.A., Hernández, E. and León, M. (2002). Optical functions of chalcopyrite $CuGa_xIn_{1-x}Se_2$ alloys. *Applied Physics A: Materials Science & Processing*, 74, 659-664.

Basore, P.A. (2006). CSG-2: Expanding the production of a new polycrystalline silicon PV technology. *Proc. of the 21st European Photovoltaic Solar Energy Conference*.

Birkmire, R.W. & Eser, E. (1997). Polycrystalline thin film solar cells: Present status and future potential, *Annu. Rev. Mater. Sc.* 27, 625.

Birkmire, R.W. (2008). Pathways to improved performance and processing of CdTe and $CuInSe_2$ based modules. C*onference Record of 33rd IEEE Photovoltaic Specialists Conference*. pp. 47-53.

Bonnet, D. (2001). Cadmium telluride solar cells. In: *Clean Electricity from Photovoltaics*. Ed. By M.D. Archer and R. Hill. Imperial College Press, New York. pp. 245-275.

Bonnet, D., Oelting, S., Harr, M., Will, S. (2002). Start-up and operation of an integrated 10MWp thin film PV module factory. *Proceedings of the 29th IEEE Photovoltaic Specialists Conference*, pp. 563–566.

Bonnet, D. (2003). Cadmium telluride thin-film PV modules. in: *Practical Handbook of Photovoltaics: Fundamentals and Applications*, edited by T. Markvart and L. Castaner, (Elseiver, New York,). p. 333-366.

Britt, J. & Ferekides, C. (1993). Thin Film CdS/CdTe Solar Cell with 15.8% efficiency. *Appl. Phys. Lett*. 62, 2851-2852.

Carlson, D.E. & Wronski, C.R. (1976). Amorphous silicon solar cell. *Appl. Phys. Lett*. 28, 671-672

Chamberlain, G.A. (1983). Organic solar cells: a review. *Solar Cells,* 8, 47-83.

Chiba, Y.; Islam, A.; Watanabe, Y.; Koyama, R.; Koide, N.; & Han, L. (2006). Dye-Sensitized Solar Cells with Conversion Efficiency of 11.1% *Jpn. J. Appl. Phys*. 45, L638-L640.

Chu, T.L, Chu, S., Lin, S., Yue, J. (1984). Large Grain Copper Indium Didiselenide Films. *J. Electrochemical Soc*. 131, 2182-2185.

Contreras, M.A., Egaas, B., Ramanathan, K., Hiltner, J., Swartzlander, A., Hasoon, F., Noufi, R. Progress towards 20% efficiency in Cu(In,Ga)$Se_2$ polycrystalline thin-film solar cells. (1999). *Prog. Photovolt: Res. Appl*. 7, 311-316.

Deckman, H.W., Wronski, C.R., Witzke, H. and Yablonovitch, E. (1983). Optically enhanced amorphous silicon solar cells. *Appl. Phys. Lett*. 42, 968-970.

Deng, S. & Schiff, E.A. (2003). Amorphous Silicon–based Solar Cells. In: *Handbook of Photovoltaic Science and Engineering,* Second Edition. Edited by A. Luque and S. Hegedus. John Wiley & Sons, Ltd., pp. 505-565.

EPIA Global market outlook for photovoltaics until 2015. (2011). European Photovoltaic Industry Association. www.epia.org.

EUR 24344 PV Status Report 2010. Institute for Energy. Joint Research Centre. European Commission. (2010). http://www.jrc.ec.europa.eu.

Fahrenbruch, A. & Bube, R., (1983). *Fundamentals of Solar Cells*, 231–234, Academic Press, New York.

Faraji, M., Sunil Gokhale, Choudhari, S. M., Takwale, M. G., and S. V. Ghaisas. (1992). High mobility hydrogenated and oxygenated microcrystalline silicon as a photosensitive material in photovoltaic applications. *Appl. Phys. Lett*. 60, 3289-3291.

Ferrazza, F. (2003). Silicon: manufacture and properties. In: *Practical Handbook of Photovoltaics: Fundamentals and Applications*, edited by T. Markvart and L. Castaner (Elseiver, New York), pp. 137-154.

Fritsche, J., Kraft, D., Thissen, A., Mayer, Th., Klein & A., Jaegermann W. (2001). Interface engineering of chalcogenide semiconductors in thin film solar cells: CdTe as an example, *Mat. Res. Soc. Symp.* Proc. , 668, 601-611.

Fthenakis, V.M., Kim, H.C., and Alsema, E. (2008). Emissions from Photovoltaic Life Cycles. *Environ. Sci. Technol*. 42, 2168-2174.

Goetzberger, A. , Hebling, C. & Schock, H.-W. (2003). Photovoltaic materials, history, status and outlook. *Materials Science and Engineering* R40, 1-46.

Cohen-Solal, G., Lincot, D., Barbe, M. (1982). High efficiency shallow p(+)nn(+) cadmium telluride solar cells. in: *Photovoltaic Solar Energy Conference*; Proceedings of the 4th International Conference, 621-626.

Cooke, M. (2008). CdTe PV progresses to mass production. *Semiconductors Today*, 3, 74-77.

Grätzel, M. (2003). Dye-sensitized solar cells. *J. Photochem. Photobiol. C: Photochem. Rev*. 4, 145-153.

Gratzel, M. (2004). Conversion of sunlight to electric power by nanocrystalline dye-sensitized solar cells. *J. Photoch. & Photobiology* A164, Issue: 1-3, 3-14.

Gray, J.L., Schwartz, R.J., Lee, Y.J. (1990). Development of a computer model for polycrystalline thin-film $CuInSe_2$ and CdTe solar cells. *Annual report 1 January – 31 December 1990*. National Renewable Energy Laboratory/TP-413-4835, 1-36.

Green, M.A., Emery, K., Hishikawa, K.Y. & Warta, W. (2011). Solar Cell Efficiency Tables (version 37). *Progress in Photovoltaics: Research and Applications 19*, pp. 84-92. ISSN 1099-159X.

Guter, W., Schöne, J., Philipps, S., Steiner, M., Siefer, G., Wekkeli, A., Welser, E, Oliva, E, Bett, A., and Dimroth F.(2009). Current-matched triple-junction solar cell reaching 1.1% conversion efficiency under concentrated sunlight, *Appl. Phys. Lett*. 94, 023504 (8 pages).

Han, S.-H., Hasoon, F.S., Hermann, A.M., Levi, D.H. (2007). Spectroscopic evidence for a surface layer in $CuInSe_2$ :Cu deficiency. *Appl. Phys. Lett*. 91, 021904 (5 pages).

Haugeneder, A.; Neges, M.; Kallinger, C.; Spirkl, W.; Lemmer, U.; Feldmann, J.; Scherf, U.; Harth, E.; Gügel, A.; Müllen, K. (1999). Exciton diffusion and dissociation in conjugated polymer/fullerene blends and heterostructures. *Phys. Rev*. B., 59, 15346-15351.

Hegedus, S. & Luque, A. (2011). Achievements and Challenges of Solar Electricity from Photovoltaics. In: *Handbook of Photovoltaic Science and Engineering,* Second Edition. Edited by A. Luque and S. Hegedus. John Wiley & Sons, Ltd., pp. 2-38.

Hein, J.R., Koschinsky, A., and Halliday, A.N. (2003). Global occurrence of tellurium-rich ferromanganese crusts and a model for the enrichment of tellurium. *Geochimica et Cosmochimica Acta*, 67, 1117-1127.

http://refractiveindex.info/?group=CRYSTALS&material=a-Si.

http://www1.eere.energy.gov/solar/pdfs/solar_program_mypp_2008-2012.pdf. *Multi Year Program Plan 2008-2012*. U.S. Department of Energy.

Jager-Waldau, A. (2010). Research, Solar Cell Production and Market Implementation of Photovoltaics. *Luxembourg: Office for Official Publications of the European Union*. 120 pp.

Ji, J. J. & Shi, Z. (2002). Texturing of glass by $SiO_2$ film. *US patent* 6, 420, 647.

Jordan, J. (1993). *International Patent Application*. WO93/14524.

Kazmerski, L.L., White, F.R., and Morgan, G.K. (1976). Thin-film $CuInSe_2$/CdS heterojunction solar cells. *Appl. Phys. Lett*. 29, 268-270.

Keppner, H., Meier, J. Torres, P., Fischer, D., and Shah, A. (1999). Microcrystalline silicon and micromorph tandem solar cells. *Applied Physics A: Materials Science & Processing*. 69, 169-177.

King, R. (2008). Multijunction cells: record breakers, *Nature Photonics*, 2, 284– 285.

Kosyachenko, L.A., Maslyanchuk, O.L., Motushchuk, V.V., Sklyarchuk, V.M. (2004). Charge transport generation-recombination mechanism in Au/n-CdZnTe diodes. *Solar Energy Materials and Solar Cells*. 82, 65-73.

Kosyachenko, L.A., Grushko, E.V., Savchuk, A.I. (2008). Dependence of charge collection in thin-film CdTe solar cells on the absorber layer parameters. *Semicond. Sci. Technol*. 23, 025011 (7pp).

Kosyachenko, L., Lashkarev, G., Grushko, E., Ievtushenko, A., Sklyarchuk, V., Mathew X., and Paulson, P.D. (2009). Spectral Distribution of Photoelectric Efficiency of Thin-Film CdS/CdTe Heterostructure. *Acta Physica Polonica*. A 116 862-864.

Kosyachenko, L.A., Savchuk, A.I., Grushko, E.V. (2009). Dependence of the efficiency of a CdS/CdTe solar cell on the absorbing layer's thickness. *Semiconductors*, 43, 1023-1027.

Kosyachenko, L.A., Grushko, E.V. (2010). Open_Circuit Voltage, Fill Factor, and Efficiency of a CdS/CdTe Solar Cell. *Semiconductors*, 44, 1375–1382.

Kuwano, Y., Ohniishi, Nishiwaki, H., Tsuda, S., Fukatsu, T., Enomoto, K., Nakashima, Y., and Tarui, H. (1982). Multi-Gap Amorphous Si Solar Cells Prepared by the Consecutive, Separated Reaction Chamber Method. *Conference Record of the 16th IEEE Photovoltaic Specialists Conference*, (San Diego, CA, 27-30.9.1982), pp. 1338-1343.

Lavagna, M., Pique, J.P. & Marfaing, Y. (1977). Theoretical analysis of the quantum photoelectric yield in Schottky diodes, *Solid State Electronics*, 20, 235-240.

Loferski, J.J. (1956). Theoretical Considerations Governing the Choice of the Optimum Semiconductor for Photovoltaic Solar Energy Conversion. *J. Appl. Phys*. 27, 777-784.

Mauk, M., Sims, P., Rand, J., and Barnett. (2003). A. Thin silicon solar cells In: *Practical Handbook of Photovoltaics: Fundamentals and Applications*, edited by T. Markvart and L. Castaner (Elseiver, New York), p. 185-226.

Meier, J., Flückiger, R., Keppner, H., and A. Shah. (1994). Complete microcrystalline p-i-n solar cell—Crystalline or amorphous cell behavior? *Appl. Phys. Lett.* 65, 860-862.

Meier, J., Dubail, S., Fischer, D., Anna Selvan, J.A., Pellaton Vaucher, N., Platz, Hof, C., Flückiger, R., Kroll, U., Wyrsch, N., Torres, P., Keppner, H., Shah, A., Ufert, K.-D. (1995). The 'Micromorph' Solar Cells: a New Way to High Efficiency Thin Film Silicon Solar Cells. *Proceedings of the 13th EC Photovoltaic Solar Energy Conference*, Nice, pp. 1445–1450.

Meier, J., Dubail, S., Cuperus, J., Kroll, U., Platz, R., Torres, P., Anna Selvan, J.A., Pernet, P., Beck, N., Pellaton Vaucher, N., Hof, Ch., Fischer, D., Keppner, H., Shah, A. (1998). Recent progress in micromorph solar cells. *J. Non-Crystalline Solids*. 227–230, 1250–1256.

Meyers, P.V. & Albright, S.P. (2000). Technical and Economic opportunities for CdTe PV at the turn of Millennium. *Prog. Photovolt.: Res. Appl*. 8, 161-169.

Mickelsen, RA. & Chen, W.S. (1981). Development of a 9_4% efficient thin-film $CuInSe_2$/CdS solar cell. *Proc.15th IEEE Photovoltaic Specialists Conference*, New York,; 800–804.

Muller, R.S. & Zuleeg, R. (1964). Vapor-Deposited, Thin-Film Heterojunction Diodes. *J. Appl. Phys*. 35, 1550-1558.

Multi Year Program Plan 2008-2012. U.S. Department of Energy. http://www1.eere.energy.gov/ solar/pdfs/solar_program_mypp_2008-2012.pdf

Minilya-Arroyo, J., Marfaing, Y., Cohen-Solal, G., Triboulet, R. (1979). Electric and photovoltaic properties of CdTe p-n homojunctions. *Sol. Energy Mater*. 1, 171-180.

Nakada, T. & Mise, T. (2001). High-efficiency superstrate type cigs thin film solar cells with graded bandgap absorber layers. *Proceedings of the 17th European Photovoltaic Solar Energy Conference*, Munich. 1027–1030.

Nishitani, M., Negami, T., Kohara, N., and Wada, T. (1997). Analysis of transient photocurrents in Cu(In,Ga)Se2 thin film solar cells. *J. Appl. Phys*. 82, 3572-3575.

Neumann, H., Tomlinson, R.D. (1990). Relation between electrical properties and composition in $CuInSe_2$ single crystals. *Sol. Cells*. 28, 301-313.

Ohnesorge, B., Weigand, R., Bacher, G., Forchel, A., Riedl, W., and Karg, F. H. (1998). Minority-carrier lifetime and efficiency of Cu(In,Ga)$Se_2$ solar cells. *Appl. Phys Lett*. 73, 1224-1227.

O'Regan, B. & Grätzel, M. (1991). A Low-Cost, High-Efficientcy Solar-Cell Based on Dye-Sensitized Colloidal $TiO_2$ Films, *Nature*, 353, No. 6346, 737-740.

Paulson, P.D. , Birkmire, R.W. and Shafarman, W.N. (2003). Optical Characterization of $CuIn_{1-x}Ga_xSe_2$ Alloy Thin Films by Spectroscopic Ellipsometry. *J. Appl. Phys*., 94, 879-888.

Repins, I., Contreras, M.A., Egaas, B., DeHart, C., Scharf, J., Perkins, C.L., To, B., and Noufi. R. (2008). 19 9%-efficient ZnO/CdS/$CuInGaSe_2$ solar cell with 81.2% fill factor. *Progress in Photovoltaics: Research and Applications*. 16, 235–239.

Romeo, A., M. Terheggen, Abou-Ras, D., Bőtzner, D.L., Haug, F.-J., Kőlin, M., Rudmann, D., and Tiwari, A.N. (2004). Development of Thin-film Cu(In,Ga)$Se_2$ and CdTe Solar Cells. *Prog. Photovolt: Res. Appl*.;12, 93–111.

Spear, W.E. & Le Comber, P.G. (1975). Substitutional doping of amorphous silicon. *Solid State Commun*. 17, 1193-1196.

Schmid, D., Ruckh, M., Grunvald, M., Schock. H. (1993). Chalcopyrite/defect chalcopyrite heterojunctions on the basis $CuInSe_2$. *J. Appl. Phys*. 73, 2902-2909.

Schroeder, D.J., Rockett, A.A. (1997). Electronic effects of sodium in epitaxial $CuIn_{1-x}Ga_xSe_2$. *J. Appl. Phys.* 82, 4982-4985.

Shafarman, W.N. & Stolt, L. (2003). Cu(InGa)Se2 Solar Cells. In: *Handbook of Photovoltaic Science and Engineering*, Second Edition. Edited by A. Luque and S. Hegedus. John Wiley & Sons, Ltd., pp. 567-616.

Sah C., Noyce R. & Shockley W. (1957). Carrier generalization recombination in p-n junctions and p-n junction characteristics, *Proc. IRE*. 45, 1228–1242.

Shah, J., Meier, A., Buechel, A., Kroll, U., Steinhauser, J., Meillaud, F., Schade, H. (2006). Towards very low-cost mass production of thin-film silicon photovoltaic (PV) solar modules on glass. *Thin Solid Film*. 502, 292-299.

Shay, J.L., Wagner, S., and Kasper, H.M. (1975). Efficient $CuInSe_2$/CdS solar cells. *Appl. Phys. Lett*. 27, 89-90.

Staebler, D.L. & Wronski, C.R. (1977). Reversible conductivity changes in discharge-produced amorphous Si. *Appl. Phys. Lett.* 31, 292-294.

Standard of International Organization for Standardization ISO 9845-1:1992. Reference solar spectral irradiance at the ground at different receiving conditions.

Sze, S. (1981). *Physics of Semiconductor Devices,* 2nd ed. (Wiley, New York).

Szlufcik, J., Sivoththaman, S., Nijs, J.F., Mertens, R.P., and Overstraeten, R.V. (2003). Low cost industrial manufacture of crystalline silicon solar cells. In: *Practical Handbook of Photovoltaics: Fundamentals and Applications*, edited by T. Markvart and L. Castaner (Elseiver, New York), pp. 155-184.

Tang, C.W. (1986). 2-Layer Organic Photovoltaic Cell. *Appl. Phys. Lett.*, 48, 183-185.

Tiwari, A.N., Krejci, M., Haug, F.-J., Zogg, H. (1999). 12_8% Efficiency Cu(In, Ga)$Se_2$ solar cell on a flexible polymer sheet. *Progress in Photovoltaics: Research and Applications*. 7, 393–397.

Tuttle, J.R., Szalaj, A., Keane, J.A. (2000). 15_2% AMO/1433 W/kg thin-film Cu(In,Ga)$Se_2$ solar cell for space applications. *Proceedings of the 28th IEEE Photovoltaic Specialists Conference*, pp. 1042–1045.

Von Roedern, B., Kroposki, B., Strand, T. and Mrig, L. (1995). *Proccedings of the 13th European Photovoltaic Solar Energy Conference.* p. 1672-1676.

Von Roedern, B. & del Cueto, J.A. (2000). Model for Staebler-Wronski Degradation Deduced from Long-Term, Controlled Light-Soaking Experiments. *Materials Research Society's Spring Meeting*. San Francisco, California, April 24-28, 2000. 5 pages.

Von Roedern, B. (2006). Thin-film PV module review: Changing contribution of PV module technologies for meeting volume and product needs. *Renewable Energy Focus*. 7, 34-39.

Wagner, S., Shay, J. L., Migliorato, P., and Kasper, H.M. (1974). $CuInSe_2$/CdS heterojunction photovoltaic detectors. *Appl. Phys. Lett*. 25, 434-435.

Widenborg, P.I. & Aberle, A.G. (2007). Polycrystalline Silicon Thin-Film Solar Cells on AIT-Textured Glass Superstrates. *Advances in OptoElectronics*. 24584 (7 pages).

Wu, X., Kane, J.C., Dhere, R.G., DeHart, C., Albin, D.S., Duda, A., Gessert. T.A., Asher, S., Levi. D.H., Sheldon, P. (2002). 16.5% Efficiency CdS/CdTe polycristalline thin-film solar cells. *Proceedings of the 17th European Photovoltaic Solar Energy Conference and Exhibition*, Munich, 995–1000.

www.firstsolar.com/recycling.

Yang, J, Banerjee, A, Guha, S. (1997). Triple-junction amorphous silicon alloy solar cell with 14.6% initial and 13.0% stable conversion efficiencies. *Appl. Phys. Lett*. 70, 2975-2977.

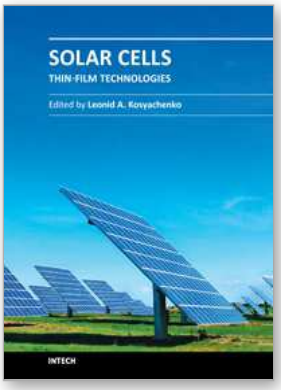


**Solar Cells - Thin-Film Technologies**

Edited by Prof. Leonid A. Kosyachenko

ISBN 978-953-307-570-9
Hard cover, 456 pages
**Publisher** InTech
**Published online** 02, November, 2011
**Published in print edition** November, 2011

The first book of this four-volume edition is dedicated to one of the most promising areas of photovoltaics, which has already reached a large-scale production of the second-generation thin-film solar modules and has resulted in building the powerful solar plants in several countries around the world. Thin-film technologies using direct-gap semiconductors such as CIGS and CdTe offer the lowest manufacturing costs and are becoming more prevalent in the industry allowing to improve manufacturability of the production at significantly larger scales than for wafer or ribbon Si modules. It is only a matter of time before thin films like CIGS and CdTe will replace wafer-based silicon solar cells as the dominant photovoltaic technology. Photoelectric efficiency of thin-film solar modules is still far from the theoretical limit. The scientific and technological problems of increasing this key parameter of the solar cell are discussed in several chapters of this volume.



INTECH
open science | open minds

**InTech Europe**
University Campus STeP Ri
Slavka Krautzeka 83/A
51000 Rijeka, Croatia
Phone: +385 (51) 770 447
Fax: +385 (51) 686 166
www.intechopen.com

**InTech China**
Unit 405, Office Block, Hotel Equatorial Shanghai
No.65, Yan An Road (West), Shanghai, 200040, China
中国上海市延安西路65号上海国际贵都大饭店办公楼405单元
Phone: +86-21-62489820
Fax: +86-21-62489821